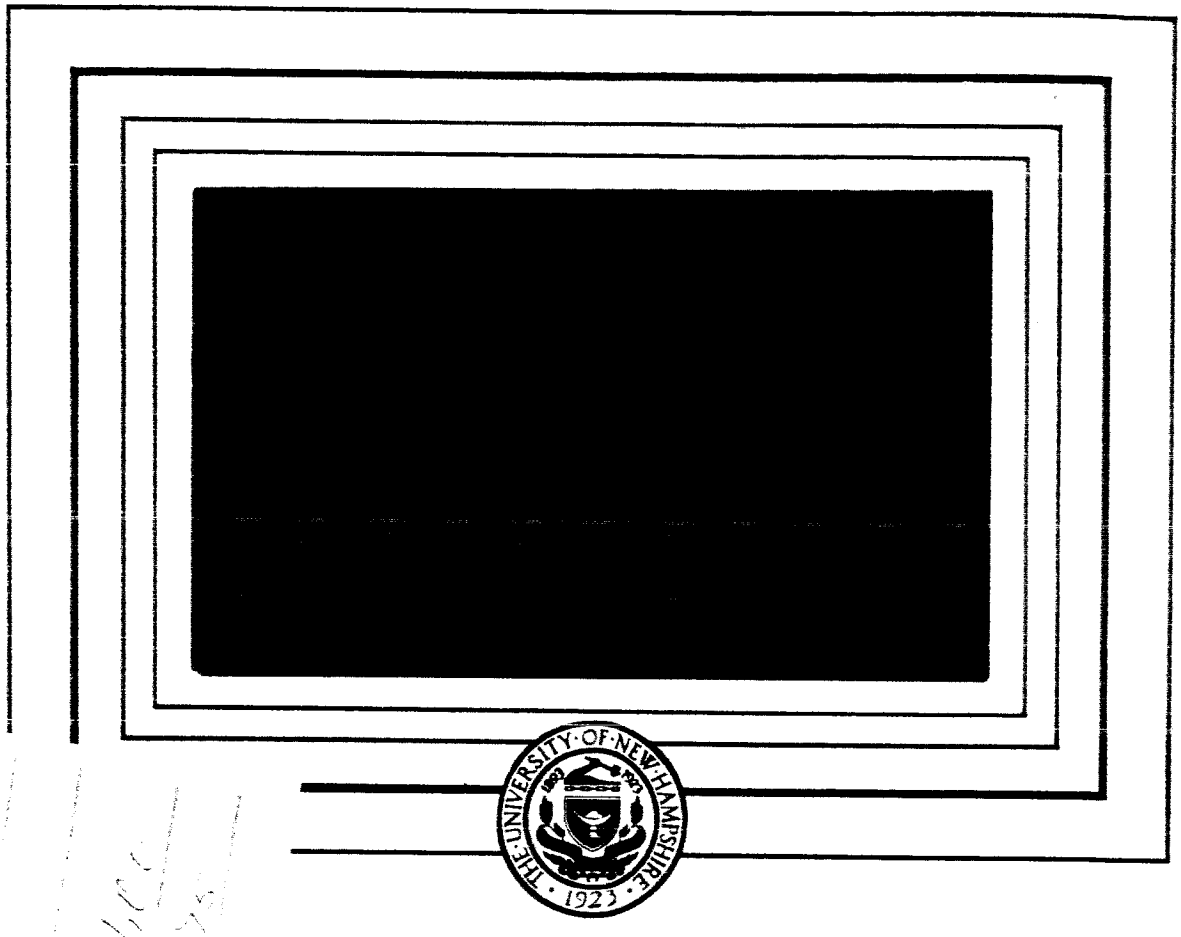

Department of Physics

UNIVERSITY OF NEW HAMPSHIRE

Durham

VIOLATION OF THE SECOND AND THIRD ADIABATIC INVARIANTS BY HYDROMAGNETIC WAVES

BY

BARNEY JAY CONRATH

B. A., Culver-Stockton College, 1957

M. A., State University of Iowa, 1959

A THESIS

Submitted to the University of New Hampshire

In Partial Fulfillment of

The Requirements for the Degree of

Doctor of Philosophy

Graduate School

Department of Physics

October, 1965

TABLE OF CONTENTS

LIST OF FIGURES

AN ABSTRACT OF

VIOLATION OF THE SECOND AND THIRD ADIABATIC INVARIANTS BY HYDROMAGNETIC WAVES

Mechanisms which violate the adiabatic invariants of the geomagnetically trapped particle motion can produce a marked influence on the spatial and temporal behavior of the particles. In this study two acceleration mechanisms are considered: violation of the second adiabatic invariant by small amplitude hydromagnetic waves and violation of the third adiabatic invariant by hydromagnetic waves of a large spatial scale.

Preliminary to the study, a review is given of the treatment of the motion of a charged particle in an electromagnetic field by means of the Alfvèn perturbation method, along with a summary of the current experimental data available on the trapped particle regime. Larmor frequencies, bounce periods, and drift periods for a range of energies and L-values are given.

Violation of the second invariant is investigated, using a simplified model of converging field lines. A restriction imposed in a previous, similar study, that the bounce period be less than the wave period, has been removed in this study. Expressions for characteristic lifetimes and diffusions have been obtained and numerical examples are given.

Violation of the third invariant by large scale magnetic disturbances with a sinusoidal dependence is investigated, using an image dipole model. Characteristic diffusion times are derived and the formulation is applied to an example of electrons with energies greater than 1.6 Mev at $L = 4$. The sinusoidal model is also compared with the sudden disturbance models of previous studies.

The results of the studies are used to define measurements which could be employed to study the specific mechanisms experimentally. The calculations of this study are primarily intended to be used as tools in the correlation of particle data with magnetic field data.

ACKNOWLEDGEMENTS

The author wishes to express his indebtedness to Dr. Richard Kaufmann of the University of New Hampshire who suggested this study and provided continued guidance throughout the course of the work. Thanks are also due to Dr. L. J. Cahill, Jr., of the University of New Hampshire for many valuable comments and discussions.

This work was performed while the author was on leave from the Goddard Space Flight Center, Greenbelt, Maryland, and was supported in part by the National Aeronautics and Space Administration under Grant NsG-624.

CHAPTER I

INTRODUCTION

A. Statement of the Problem

Since the discovery of the geomagnetically trapped energetic particles (Van Allen, et al., 1958), a considerable amount of experimental data has been acquired on their composition, energy, and spatial distribution. As the available data have increased, questions have naturally arisen as to the origin of the particles, their relation to the cosmic radiation and to the interplanetary medium, and the acceleration and loss mechanisms which, along with source mechanisms, determine their energy spectra and their spatial distribution.

In this study we shall be concerned primarily with acceleration and loss mechanisms. A number of such mechanisms have been proposed, including interaction of the energetic particles with the background thermal particles through charge exchange and Coulomb scattering, interaction with electromagnetic radiation, large-scale convective motions of the thermal plasma and field lines, and acceleration through interactions with hydromagnetic disturbances. A number of the mechanisms which have been proposed require rather special sets of circumstances in order to operate effectively. We shall consider two types of interactions with hydromagnetic disturbances which must occur, at least to some extent, whenever such disturbances are present. These mechanisms

include violation of the second adiabatic invariant by small-amplitude hydromagnetic waves and violation of the third adiabatic invariant by small-amplitude magnetic disturbances existing on a large spatial scale. The first of these mechanisms produces second order Fermi acceleration, resulting in migration of particle mirror points down magnetic field lines and eventual loss of particles into the atmosphere. The principal effect of the second mechanism is to produce a radial diffusion of particles across magnetic shells.

We shall begin by briefly reviewing the fundamental concepts of the motion of a charged particle in an electromagnetic field. The experimental data currently available on the trapped particle regime will be reviewed along with other properties of the magnetosphere. A summary of acceleration mechanisms which may be operative in the magnetosphere will be given, and the propagation of hydromagnetic disturbances will be discussed. Preliminary to the main study, the fundamental periods of the trapped particle motion will be discussed, and a tabulation of these parameters will be given. The violation of the second and third invariants will be investigated with an effort being made to carry out quantitative calculations which will indicate the characteristics of the disturbances which are necessary for these mechanisms to be effective. The results of these calculations will be employed to define measurements which could be used to study the mechanisms experimentally.

B. Properties of the Magnetosphere

The term "magnetosphere," originally proposed by Gold (1959), is generally used to refer to that region of space which is under the direct influence of the earth's magnetic field. In the past several years a picture of the general shape of this region has emerged. The shape of the magnetosphere is highly influenced by the solar wind, a plasma flow issuing from the sun with a directed velocity of several hundred km/sec and a density of the order of 10 cm^{-3}. (Parker, 1960a; Obayashi, 1964). The effect of this plasma flow as it impinges on the geomagnetic field is to confine the field to a rather well-defined cavity (Johnson, 1960). Observational evidence indicates that the boundary of this cavity, during magnetically quiet periods, is located at about 10 earth radii in the vicinity of the earth-sun line, increasing to larger distances away from local noon (Cahill and Amazeen, 1963). Detailed theoretical calculations of the shape of the magnetosphere have been made leading to a fairly complete picture on the sunward side of the earth (Beard, 1964; Mead and Beard, 1964). Details of the topology of the nighttime side are less well known, due both to a lack of observational data and to theoretical difficulties (Alfven, 1963). Present models range from those with tails which close at several earth radii to those with open tails extending as far as 20 to 50 astronomical units (Dessler, 1964). Due to the "supersonic" nature of the plasma flow, a collisionless shock front apparently exists, extending 3 or 4 earth radii outside the boundary in the vicinity of the earth-sun line.

The geomagnetically trapped energetic particles located

within the magnetosphere originally were assumed to occupy two more or less distinct zones, with the energetic component of the inner zone being mostly protons and that of the outer zone being mostly electrons. However, both electrons and protons are found throughout the trapping region. Typical electron fluxes in the heart of the outer zone (3.5 to 4 earth radii) are (Frank et al., 1964)

$$J\ (E>40\ \text{kev}) = 3 \times 10^{7}\ (\text{cm}^2\ \text{sec})^{-1}$$
$$J\ (E>230\ \text{kev}) = 3 \times 10^{6}\ (\text{cm}^2\ \text{sec})^{-1}$$
$$J\ (E>1.6\ \text{Mev}) = 3 \times 10^{5}\ (\text{cm}^2\ \text{sec})^{-1}$$

Directional intensities and spectra of protons from 100 kev to 4.5 Mev have been obtained by Davis et al. (1962). Peak intensities of 6×10^{7} protons/cm^2-sec-ster were found with energy spectra approximated by $e^{-E/Eo}$ with Eo values of 400, 120, and 64 kev at 2.8, 5.0 and 6.1 earth radii respectively

The properties of the inner trapping regions remain fairly constant with time, while the outer trapping regions undergo considerable temporal variation, much of which is correlated with solar activity.

In order to formulate quantitative theories of the formation of the radiation belts and their variation with time, a firm understanding of the mechanisms whereby energy is transferred from interplanetary space into the magnetosphere is necessary. At the present time such an understanding is lacking. One group of such mechanisms might be classified as direct, while a second class of mechanisms operates in the boundary regions of the magnetosphere, and a third class occurs locally within the magnetosphere.

One mechanism belonging to the direct type is the energetic proton flux resulting from the decay of albedo neutrons from galactic cosmic ray events (Lenchek and Singer, 1962). Another mechanism of this type consists of the injection of energetic particles from the interplanetary plasma directly into the magnetosphere, either by diffusion across the boundary or by the intrusion of tongues of plasma into the magnetosphere.

The remaining two classes of energy transfer mechanisms involve the acceleration of low-energy particles already within the magnetosphere. Various examples of the mechanisms of this type will be considered below.

Another property of the magnetosphere which may be of some importance in the acceleration of particles is its apparent capability of undergoing convective motion. Gold (1959) pointed out a criterion for stability against convection, analogous to the adiabatic lapse rate in the lower atmosphere and concluded that convection could possibly occur in certain regions of the magnetosphere. Axford and Hines (1961) extended this idea and proposed a convective model whereby particles could be carried downward from the boundary.

The existence of hydromagnetic waves propagating in the earth's field was predicted a number of years ago and has been confirmed experimentally in recent years. They apparently are generated at the boundary of the magnetosphere and also possibly within the magnetosphere (Patel, 1964). These waves may play an important role in the acceleration and scattering of particles.

C. Individual Particle Motion and the Guiding Center Approximation

The motion of a particle in an electromagnetic field is governed by the well-known Lorentz force equation

$$m \frac{dv}{dt} = e(\underline{E} + \frac{1}{c} \underline{v} \times \underline{B}) \qquad (1.1)$$

where m is the particle mass, e is the charge on the particle, $\underline{v}$ is the particle velocity, c is the speed of light, $\underline{E}$ is the electric field strength, and $\underline{B}$ is the magnetic flux density. When the electric and magnetic fields vary in space and time, the solutions to (1.1) can be quite complicated. One important property of the motion can be obtained quite simply, however, by noting that the magnetic part of the Lorentz force is always perpendicular to the direction of motion and therefore the magnetic field can do no work on the particle, so changes in the kinetic energy must be due to the presence of the E-field. Thus, in the absence of an electric field, the kinetic energy is a constant of the motion which implies that the speed of the particle remains constant.

There are two general methods for treating the motion of a particle in a magnetic field. One method is to attempt to integrate (1.1) numerically and obtain the trajectory of the particle in detail. This approach has been discussed extensively by Störmer (1955) and is well-suited for particles such as high-energy cosmic rays which make only a few gyrations in the spatial volume under consideration. The second method consists of following the so-called "guiding center" motion of the particle and is well-suited for describing the motion of low-energy particles in the geomagnetic field. Thus, the two methods tend to complement one another. It is the latter method, developed originally by

Alfvén (1963), which we wish to consider.

A review of the guiding center method has been given by Northrop (1963a), and we shall follow his development. Let us first consider the motion of a particle in a uniform field, in which case the behavior is well-known and consists of a circular gyration in a plane perpendicular to the field lines with a superposed constant motion parallel to the field lines. The gyration frequency is given by

$$\omega_L = \frac{eB}{mc} \tag{1.2}$$

and is called the Larmor frequency of the particle. The radius of curvature of the trajectory projected onto a plane perpendicular to the lines of force is called the Larmor radius and is given by $\rho = v_\perp / \omega_L$ where $v_\perp$ is the component of particle velocity perpendicular to $\underline{B}$. Now if we consider a magnetic field which is non-uniform, but varies sufficiently slowly so that it does not change appreciably over distances of the order of ρ, then the lowest order approximation can be taken to be the circular gyration about the lines of force. The effects of the non-uniformity of the magnetic field can be introduced as perturbations and first order corrections to the motion can be introduced by considering the effects of the perturbations on the motion of the center of gyration or the "guiding center." Other effects, such as an electric field and a time variation in the magnetic field, can be introduced as perturbations also if these effects are sufficiently small.

Let us consider a particle whose instantaneous position is $\underline{r}$ with its guiding center located at $\underline{R}$ as shown in Figure 1.

The position vector $\underline{r}$ can be written in terms of $\underline{R}$ and the vector Larmor radius $\underline{\rho}$ in the form

$$\underline{r} = \underline{R} + \underline{\rho} \tag{1.3}$$

The unit vector $\hat{e}_1$ lies along $\underline{B}$ with $\hat{e}_2$ and $\hat{e}_3$ in a plane perpendicular to $\underline{B}$ completing an orthogonal triade. The vector Larmor radius can be written

$$\underline{\rho} = \rho \ (\hat{e}_2 \sin \omega_L t + \hat{e}_3 \cos \omega_L t) \tag{1.4}$$

This just represents the circular motion about the guiding center.

The E- and B- fields in (1.1) are functions of $\underline{r}$ in general, so we should write

$$\ddot{\underline{r}} = \frac{e}{m} \left[\underline{E}(\underline{r}) + \frac{1}{c} \dot{\underline{r}} \times \underline{B}(\underline{r})\right] \tag{1.5}$$

If E and B do not change appreciably over distances of the order of ρ, we can replace $\underline{E}(\underline{r})$ and $\underline{B}(\underline{r})$ by $\underline{E}(\underline{R})$ and $B(\underline{R})$ plus gradient corrections such that (1.5) becomes

$$\ddot{\underline{r}} = \frac{e}{mc} \left[\dot{\underline{r}} \times \underline{B}(\underline{R}) + (\dot{\underline{r}} \times \hat{e}_1)\underline{\rho} \cdot \nabla \underline{B}\right] + \frac{e}{m} \underline{E}(\underline{R}) \tag{1.6}$$

We can use (1.3) to eliminate $\underline{r}$ from (1.6), obtaining

$$\begin{aligned} \ddot{\underline{R}} = {} & \rho \frac{\omega_L^2}{m} (\hat{e}_2 \sin \omega_L t + \hat{e}_3 \cos \omega_L t) \\ & + \frac{e}{mc} \left[\dot{\underline{R}} \times \underline{B}(R) + \dot{\underline{\rho}} \times \underline{B}(\underline{R}) \right. \\ & \left. + (\dot{\underline{R}} \times \hat{e}_1 + \underline{\rho} \times \hat{e}_1)\underline{\rho} \cdot \nabla \underline{B}\right] \\ & + \frac{e}{m} \underline{E}(\underline{R}) \end{aligned} \tag{1.7}$$

where use has been made of (1.4). Taking the time average of (1.7) over one Larmor period gives

$$\ddot{\underline{R}} = \frac{e}{mc}\left[\dot{\underline{R}} \times \underline{B}(\underline{R}) - \frac{\mu c}{e}\nabla_{\perp} B\right] + \frac{e}{m}\underline{E}(\underline{R}) \qquad (1.8)$$

where $\nabla_{\perp} B$ is the component of ∇B perpendicular to $\underline{B}$ and $\mu = m\rho^2\omega_L^2 \;/\; 2B$ is the diamagnetic moment of the particle as it gyrates in the magnetic field. This quantity will be discussed at greater length in the following section.

To obtain the drift velocity perpendicular to $\underline{B}$, we take the cross product of both sides of (1.8) with $\underline{B}(\underline{R})$. Letting $\dot{\underline{R}}_{\perp}$ denote the perpendicular drift velocity we have

$$\dot{\underline{R}}_{\perp} = \frac{mc}{e}\,\frac{\underline{B} \times \ddot{\underline{R}}}{B^2} + \frac{\mu c}{e}\,\frac{\underline{B} \times \nabla_{\perp} B}{B^2} + \frac{c\underline{E} \times \underline{B}}{B^2} \qquad (1.9)$$

The last term is just the familiar "E x B drift" and the second term is the so-called "gradient drift." The first term contains several different drift effects and must be considered further. Writing $\dot{\underline{R}}$ in terms of its components parallel and perpendicular to $\underline{B}$ and expanding the first term gives, after some algebraic manipulation,

$$\begin{aligned}\dot{\underline{R}}_{\perp} = \frac{\underline{B}}{B^2} \times \Bigg\{ & -c\underline{E} + \frac{\mu c}{e}\nabla B + \frac{mc}{e}\Bigg[v_{\parallel}^2 \frac{\partial \hat{e}_1}{\partial s} \\ & + v_{\parallel}\frac{\partial \hat{e}_1}{\partial t} + v_{\parallel}\underline{u}_E \cdot \nabla \hat{e}_1 + \frac{\partial \underline{u}_E}{\partial t} \\ & + v_{\parallel}\frac{\partial \underline{u}_E}{\partial s} + \underline{u}_E \cdot \nabla \underline{u}_E\Bigg]\Bigg\}\end{aligned} \qquad (1.10)$$

where $v_{\parallel}$ is the component of particle velocity parallel to $\underline{B}$, $\underline{u}_E = c\,\underline{E} \times \underline{B}/B^2$, and s is the distance along the field line. If the E-field and time variations in $\underline{B}$ are sufficiently small, the last five terms in (1.10) can be neglected, resulting in

$$\dot{\underline{R}}_{\perp} = \frac{\underline{B}}{B^2} \times \left[-c\,\underline{E} + \frac{\mu c}{e}\nabla B + \frac{mc}{e}v_{\parallel}^2\,\frac{\partial \hat{e}_1}{\partial s}\right] \qquad (1.11)$$

This is the form frequently found in the literature. The terms in (1.11) have simple physical interpretations. The gradient drift term arises when we have a situation similar to that shown in the diagram below. The B-field is directed

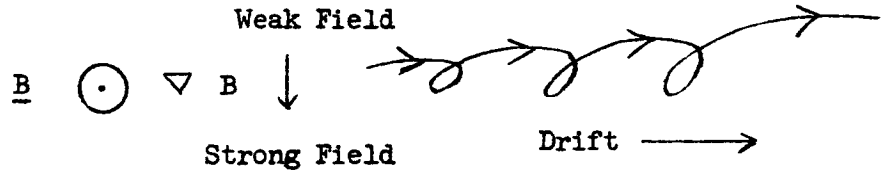

out of the page. As the particle spirals about a line of force, the instantaneous Larmor radius will be large in the weak part of the field and small in the strong part, so the particle executes a motion like that shown in the diagram, which constitutes a drift of the guiding center in a direction perpendicular to both $\underline{B}$ and ∇B. The direction of the drift shown in the diagram is for a positively charged particle. A negatively charged particle would drift in the opposite direction. The last term in (1.11) is the "line curvature drift." This drift is the result of an inertial force set up as the guiding center moves along a curved field line as shown in the diagram below. R is the instantaneous radius of curvature of the field line.

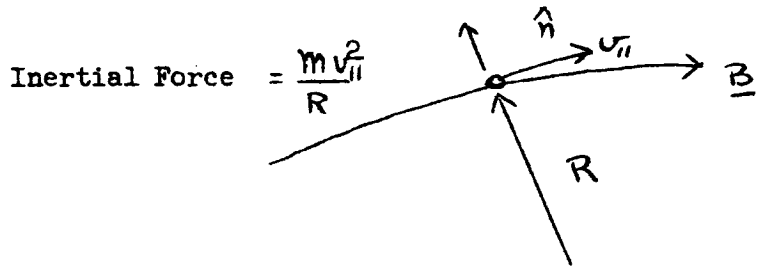

The inertial force $mv_{\parallel}^2/R$ acts in a direction normal to the field line in the direction of the unit vector $\hat{n}$. The particle would experience the same force if the field line were straight

and an effective electric field were introduced with a strength given by

$$\underline{E}\ \text{eff} = \frac{m v_{\parallel}^2}{eR}\,\hat{n} \tag{1.12}$$

This effective E-field would produce an E x B drift

$$\underline{v}_E = c\,\frac{\underline{E}\ \text{eff} \times \underline{B}}{B^2} = \frac{mc}{e}\,v_{\parallel}^2\ \frac{\hat{n}}{R} \times \frac{B}{B^2} \tag{1.13}$$

Since $\hat{n} / R = \partial \hat{e}_1 / \partial s$, this is just the line curvature drift term of (1.11).

The equation of motion of the guiding center parallel to the line of force can be obtained by taking the scalar product of both sides of (1.8) with $\hat{e}_1$. This results in

$$\frac{dv_{\parallel}}{dt} = \frac{e}{m} E_{\parallel} - \frac{\mu}{m}\frac{\partial B}{\partial s} + \underline{\mu}\ \underline{E}\ \frac{d\hat{e}_1}{dt} \tag{1.14}$$

The second term on the right-hand side of (1.14) is the so-called mirror term. To see the significance of this term, let us consider the case when the electric field vanishes and $\partial B/\partial s$ is a constant. It will be shown in the following section that μ is an approximate constant of the motion. Using this fact, a first integral of (1.14) can be obtained in the form

$$v_{\parallel}\ (t) = v_{o_{\parallel}} - \mu\,\frac{\partial B}{\partial s}\,t \tag{1.15}$$

where $v_{o_{\parallel}}$ is the particle velocity at time t = 0. Thus, as the particle moves into a region of increasing field strength, its guiding center will stop and reverse its direction. The

particle is in effect reflected. A magnetic field configuration with converging field lines is referred to as a "magnetic mirror." Equations (1.11) and (1.14) provide a complete description of the guiding center motion of the particle.

D. The Adiabatic Invariants

The main features of the motion of charged particles in non-uniform magnetic fields can generally be well described in terms of the so-called adiabatic invariants. These are parameters of the motion which generally remain constant even when the field seen by the particle is slowly varying. The concept of adiabatic invariants was first used in the perturbation theory of celestial mechanics, and it was later employed in the "old" quantum theory, where the quantized quantities were the action integrals which are adiabatic invariants.

In general the number of adiabatic invariants associated with a mechanical system is less than or equal to the number of degrees of freedom of the system. In particular, the motion of a particle in a dipole-like field such as the unperturbed field of the earth will have three adiabatic invariants associated with it. We shall now consider each invariant separately.

1. First Invariant or Magnetic Moment. It can be shown that the magnetic moment μ of the current loop due to the motion of the particle in its Larmor orbit is an invariant of the long-term motion even when we have a general time-dependent $\underline{B}$-field and (in the non-relativistic limit) when large $\underline{E}$-fields are present. The proof for the general case is quite lengthy (Northrop, 1963b), but it is rather simple for the

special case of static $\underline{B}$-fields. The latter proof will be outlined below, following Northrop (1963a).

For the case of static $\underline{B}$-fields, we know $\nabla \times \underline{E} = 0$ from Faraday's law, and $\underline{E}$ can be written as the gradient of a scalar potential ϕ. Since the magnetic field does no work on the particle, we can write the total energy of the particle in the form

$$W = (1/2) \quad (mv_{\parallel}^2 + mu_E^2) + \mu B + e\phi \tag{1.16}$$

where the term in parentheses is the energy of the guiding center motion, and μB is the energy of the particle in its Larmor orbit. In the case being considered, W is conserved, so we can write $dW/dt = 0$. Differentiating (1.16), equating the resulting expression to zero, and using the guiding center approximation (1.14) for $dv_{\parallel}/dt$ gives

$$\frac{d(\mu B)}{dt} - e\frac{d\phi}{dt} - mu_E \cdot \frac{du_E}{dt} - mv_{\parallel}\left(\frac{e}{m}E_{\parallel} - \underbrace{\frac{\mu}{m}\frac{dB}{ds}}_{=0} + \underline{u}_E \cdot \frac{d\hat{e}_{\parallel}}{dt}\right) \tag{1.17}$$

Now we can write

$$\frac{d\phi}{dt} = v_{\parallel}\frac{d\phi}{ds} + \dot{\underline{R}}_{\perp} \cdot \nabla\phi \tag{1.18}$$

Using (1.18) and the guiding center approximation (1.11) for $\dot{\underline{R}}_{\perp}$ in (1.17) gives

$$\frac{d(\mu B)}{dt} = \mu\, \underline{u}_E \cdot \nabla B + \mu v_{\parallel}\frac{dB}{ds} = \mu\frac{dB}{dt} \tag{1.19}$$

Therefore

$$\frac{d\mu}{dt} = 0 \tag{1.20}$$

The magnetic moment can be written in several other useful forms

$$\mu = \frac{P_\perp^2}{2mB} = \frac{m\,p^2 w^2}{2\,B} = \frac{e^2}{2\pi m e^2}(\pi p^2\,B) \qquad (1.21)$$

The quantity $\pi \rho^2 B$ is the magnetic flux threading through the Larmor orbit, so this quantity is also an invariant of the motion. Hence, the particle can be visualized as moving on the surface of a tube of constant flux. It should be kept in mind that the perpendicular velocity $v_\perp$ must be with reference to a frame moving with the guiding center.

The first invariant still holds in the relativistic case provided $P_\perp$ and B are taken to be the momentum and field as observed in a frame moving with velocity $\underline{u}_E$.

2. Second or Longitudinal Invariant. In the sense that the first invariant is associated with the Larmor gyration of the particle, the second invariant is associated with the oscillation of the guiding center of the particle back and forth between mirror points when such a field geometry exists. This parameter can be written

$$J = \oint p_{\parallel}\, ds \qquad (1.22)$$

where $p_{\parallel}$ is $mv_{\parallel}$, s is the distance along a line of force, and the integral is taken over a complete oscillation. In order for J to be conserved, it is necessary for the guiding center drift velocity $\dot{R}_\perp$ to be small compared to $v_{\parallel}$ so that the particle stays on essentially the same line during one "bounce" period. In general it can be shown that J is invariant, even for relativistic energies and time-varying fields, provided the period of variation is much greater than the bounce period (Northrop and

Teller, 1960). Actually, it is the value of dJ/dt averaged over one bounce period which vanishes and not its instantaneous value.

3. Third or Flux Invariant. When a particle for which J is conserved is subjected to a drift, it will move across lines of force on which J is constant. These lines will form a surface, the so-called longitudinal invariant surface. When this surface is closed, a third invariant exists. It is the magnetic flux $\oint$ linking the longitudinal invariant surface. It is obvious that $\oint$ is constant for the case of static fields, since the particle will precess repeatedly around the same surface and the surface will not change with time. If the B-field has a time dependence which is slow compared to the time it takes the particle to precess once around the surface, $\oint$ is still conserved (Northrop, 1963b).

A convenient means of describing the motion of a low-energy particle in the geomagnetic field is provided by the adiabatic invariants. When all three invariants are conserved, the particle will precess in a Larmor circle about its guiding center while the the guiding center will oscillate back and forth in latitude between mirror points, at the same time precessing around in longitude until it eventually makes a complete circuit and returns to the same line of force from which it started. If the third invariant does not hold, then the guiding center will not necessarily return to the same line after drifting around even though the particle continues to oscillate between mirror points. If the second invariant breaks down, the particle may still continue to be reflected from mirror points, but the mirror points themselves may change. If the first invariant breaks down, the particle may no longer be reflected.

In the case of motion in the geomagnetic field, the drift period will be the longest of the three, while the Larmor period will be the shortest. Thus, if we introduce a time-dependent perturbation and gradually increase the frequency of the perturbation, the third invariant would be expected to break down when the frequency of the perturbation is of the same order as the drift frequency. The second invariant will break down when the perturbation frequency reaches the vicinity of the bounce frequency. Finally, the first invariant will be violated when the perturbation frequency is approximately equal to the Larmor frequency.

The adiabatic invariants as we have defined them above are really the lowest order terms in an asymptotic series. Systematic formal analysis shows that the conserved quantities should be written (Northrop, 1963b)

$$\text{const} = a_0 + \epsilon a_1 + \epsilon^2 a_2 + \ldots$$

where ϵ is some smallness parameter and a_0 is the quantity usually referred to as "the" invariant. It should be noted that it would be possible for an invariant to be conserved to the first order but be violated at the higher orders.

E. Mechanisms for Scattering and Accelerating Trapped Particles

In this section we shall consider some of the mechanisms whereby the geomagnetically trapped radiation may undergo acceleration or scattering. In order for an irreversible acceleration of trapped particles to occur, it is necessary that one or more of the adiabatic invariants of the motion be violated. We shall

briefly review some of the investigations that have been made on the effects of the breakdown of the adiabatic invariants by various mechanisms.

The rate of change of the total kinetic energy of a particle, averaged over a gyration and assuming μ is conserved, can be written

$$\frac{dW}{dt} = e\underline{E}\,(\underline{R},t) \cdot \dot{\underline{R}} + \mu \frac{\partial B}{\partial t}(\underline{R},t) \qquad (1.23)$$

where $\dot{\underline{R}}$ is the total guiding center drift velocity $\hat{e}_{\parallel} v_{\parallel} + \dot{\underline{R}}_{\perp}$. The first term represents the change in energy due to guiding center motion in the $\underline{E}$-field. The second term is the induction term leading to "betatron" acceleration, due to the $\underline{E}$-field with non-vanishing curl acting about the circle of gyration. The reason the second term contains a partial time derivative rather than the total derivative

$$\frac{dB}{dt} = \frac{\partial B}{\partial t} + v_{\parallel} \frac{\partial B}{\partial s} + \underline{u}_E \cdot \nabla B \qquad (1.24)$$

is that magnetic field gradients do not change the total energy, but merely interchange energy between the parallel and perpendicular components as in the mirror effect (Northrop, 1963b). If the magnetic field can be uniformly increased at a rate sufficiently slow to conserve μ, then a trapped particle can receive a net energy gain.

Coleman (1961) has examined the betatron effect for relativistic particles and finds that for an isotropic flux with an energy spectrum $N(>E) = E^{\delta}$, the value of δ will increase slightly with increasing B and decrease slightly with decreasing B.

A possible means of producing betatron acceleration is provided by the convective model of Axford and Hines (1961). Particles could be carried downward from the boundary of the magnetosphere and undergo acceleration as they pass into regions of higher field strength (Kaufmann, 1963). Dessler and Karplus (1961) have suggested that changing field strength accompanying the formation of a ring current could also produce betatron acceleration. The so-called Fermi mechanism was originally suggested by Fermi (1949) in an effort to explain the acceleration of high energy cosmic ray particles in interstellar space. The principle of the method is acceleration of a particle by means of collisions with a moving mirror point in analogy with a ball being struck with a bat. In a frame of reference in which the magnetic field is static, there will appear to be no energy change when the particle is reflected, but to an observer in a "fixed" frame there may be an energy change. The energy change will be simply $2mU(v-U)$ if v is the final velocity of the particle in the fixed frame and U is the velocity of the moving frame relative to the fixed frame.

Starting with the rate of change of the energy of the particle as viewed in the fixed frame written in the form

$$\frac{dW}{dt} = e v_{\parallel} \underline{E}_{\parallel} + e\dot{\underline{R}}_{\perp} \cdot \underline{E} + \mu \frac{\partial B}{\partial t} \qquad (1.25)$$

and expressing the quantities in terms of the velocity of the moving frame $\underline{U}$, it can be shown that (Northrop, 1963b)

$$\frac{dW}{dt} = \mu U_{\parallel} \frac{\partial B}{\partial s} + m(v_{\parallel} - U_{\parallel})^2 \underline{U}_{\perp} \cdot \frac{\partial \hat{e}_1}{\partial s} \qquad (1.26)$$

It is possible to distinguish between two different types of Fermi acceleration. In the so-called "type a" accelerations, the guiding center moves along a straight line of force, and the second term in (1.26), which involves the line curvature, vanishes. If the particle guiding center moves along a curved line of force, but with the field strength constant along the line, then the first term will be zero, and this is "type b" acceleration. In going from (1.25) to (1.26) the $\mu\left(\frac{\partial B}{\partial t}\right)$ term goes into forming the $-\mu U_{\parallel}\left(\frac{\partial B}{\partial s}\right)$ term. Hence, betatron acceleration is really a part of Fermi "type a" acceleration.

Moving plasma clouds in the boundary region could produce Fermi acceleration, which would be inefficient for electrons but could be effective for protons. This process has been described by Parker (1958). The alternate raising and lowering of mirror points discussed above in connection with the breakdown of the second invariant can be viewed as a Fermi acceleration, since the particles will be reflected from moving mirror points.

The first detailed investigation of the breakdown of the third invariant appears to have been that of Parker (1960). In this study he considered only those particles with pitch angles of 90° in the geomagnetic equatorial plane. Particles of this type located at a given radial distance will simply drift around the earth on a contour of constant field strength, remaining in the equatorial plane. The unperturbed field was assumed to be that of a dipole. A geomagnetic storm-type of disturbance was simulated mathematically by considering the effects of a plane of infinite conductivity brought in from infinity. Such a perturbation will cause the field to be compressed on the side toward

the plane. If we consider a ring of particles around the earth at a given radius before the perturbation, this ring will be displaced with the field lines if the perturbation occurs slowly enough so that the first and second invariants are conserved. Each particle will try to precess along contours of the field strength in which it now finds itself. Since for a given radius on the side toward the plane the field strength will now be stronger, the contours of constant field strength are displaced toward the plane. Thus, the particles initially in a ring will be diffused into a band. By using this model, Parker was able to set up and solve a diffusion equation showing the behavior of particles subjected to a series of such perturbations.

A study similar to that of Parker was carried out by Davis and Chang (1962), using the same model but with a different diffusion equation. The results were similar, except that the density of particles at smaller radii was found to be somewhat greater. The Davis and Chang model has recently been applied to disturbances of the sudden-impulse type by Nakada and Mead (1965). These studies will be considered in greater detail in Chapter VI.

The effects of the violation of the second invariant by hydromagnetic waves have been investigated theoretically by Parker (1961a). He considers the behavior of particle motion when hm waves pass across the mirror points. The mirror points will be ascending during the part of the wave in which B is increasing and descending when B is decreasing. Thus, the particle will be reflected from moving mirror points and Fermi acceleration is possible. (The mechanism will be discussed in more detail below).

By integrating the guiding center equation (1.14) for

motion parallel to the line with simplified wave models, Parker was able to study the effects that hm waves have on the particle distributions along the lines. From this study he concluded that, for hm disturbances extending throughout the magnetosphere, the net effect is a diffusion of particles down the lines of force and loss into the atmosphere. In this study certain restrictions were imposed on the particle energies which could be treated in the presence of waves of a given frequency. One of our objectives in the study presented in Chapter III is to remove these restrictions.

The effects of both hydromagnetic disturbances and electromagnetic radiation on the first invariant have been investigated by a number of authors. In order to be effective in breaking down the first invariant, a perturbation must have a time scale of the same order as the Larmor period of the particle.

Studies of the effects of small transverse perturbations to an otherwise uniform field have been made by Wentzel (1961a; 1961b; 1962) and Parker (1964). In both cases it was found that the amount of scattering introduced is quite sensitive to the number of reverse bends in the disturbance traversed by the particle during one Larmor period. Since the maximum frequency of hm waves which will propagate is equal to the local ion cyclotron frequency, we would not expect hm waves to be effective in breaking down the first invariant in the electron belt. However, there is a chance for some effect in the proton belt, especially for the case of waves which may be "Doppler shifted" up to the proton Larmor frequency by the motion of the proton toward oncoming waves. This possibility has been investigated by Dragt (1961) by introducing hm waves as perturbation to a dipole field. He finds that this

may be an effective mechanism in causing energetic protons at distances greater than two earth radii to diffuse down the field lines into the atmosphere.

The effectiveness in breaking down the first invariant by electromagnetic waves in the whistler range propagating in the magnetosphere has been considered by several authors. Helliwell and Bell (1960) have suggested acceleration of electrons by whistlers with the generally descending frequency of the whistlers keeping in step with the electron gyration frequency which will be decreasing as the relativistic mass increases. The method has been re-examined by Parker (1961b), who concludes that the method is inefficient unless the whistler field amplitudes are greater than 10^{-2} volt/meter. He has extended the study to include transresonant acceleration, in which the whistler frequency sweeps through the electron gyration frequency, and he finds that electron velocities may be scattered by this mechanism. Similar investigations have been carried out by Dungey (1963) and Cornwall (1964).

A mechanism has been described by Dungey (1958) whereby a neutral line (of zero B field) is set up between two points in the presence of an electric field. A discharge could then take place, resulting in particle acceleration. The first invariant will not be conserved in the vicinity of a neutral point or a neutral line, so scattering can occur.

CHAPTER II

FUNDAMENAL PERIODS OF THE TRAPPED PARTICLE MOTION

Since violation of an adiabatic invariant can occur when perturbations exist with periods comparable to the period of motion associated with the invariant, it is useful to begin the study by making a tabulation of the fundamental periods of the motion. In particular, we are interested in the three fundamental periods of both trapped electrons and protons over a wide energy range and for L-values out to L=10.

A. Larmor Frequency

The Larmor frequency ν of a charged particle spiraling about a line of force is easily calculated, using the relation

$$\nu = \frac{1}{2\pi} \frac{eB}{\gamma mc} \tag{2.1}$$

where γ is the relativistic mass ratio $\left(1 - \frac{v^2}{c^2}\right)^{-\frac{1}{2}}$. Since B changes as the guiding center of the particle moves along a line of force, ν changes, having a maximum value at the mirror points and a minimum value at the equatorial plane. For the purpose of this and the following calculations, we shall assume as a magnetic field model an earth-centered dipole with a field strength of 0.312 gauss at the surface of the earth at the magnetic equator.

Values of ν at the equatorial plane are given for electrons and protons in Table I. Assuming conservation of the first invariant, ν at the mirror points can be obtained by dividing the values given in Table I by $\sin^2 \alpha$ where α is the equatorial pitch angle of the particle. For example, a particle with a pitch angle of thirty degrees will have a value of ν at the mirror points four times the value at the equator. The decrease in the Larmor frequencies of

TABLE I

LARMOR FREQUENCIES AT THE EQUATOR

ENERGY \ L	2	3	4	5	6	8	10
Protons							
0.1 ev	62.5 cps	18.5 cps	7.9 cps	4.0 cps	2.3 cps	0.99 cps	0.5 cps
1.0 "	62.5 "	18.5 "	7.9 "	4.0 "	2.3 "	0.99 "	0.5 "
10 "	62.5 "	18.5 "	7.9 "	4.0 "	2.3 "	0.99 "	0.5 "
100 "	62.5 "	18.5 "	7.9 "	4.0 "	2.3 "	0.99 "	0.5 "
1 kev	62.5 "	18.5 "	7.9 "	4.0 "	2.3 "	0.99 "	0.5 "
10 "	62.5 "	18.5 "	7.9 "	4.0 "	2.3 "	0.99 "	0.5 "
100 "	62.5 "	18.5 "	7.9 "	4.0 "	2.3 "	0.99 "	0.5 "
1 Mev	62.5 "	18.5 "	7.9 "	4.0 "	2.3 "	0.99 "	0.5 "
10 "	62.5 "	18.5 "	7.9 "	4.0 "	2.3 "	0.99 "	0.5 "
Electrons							
0.1 ev	112 kc	32.9 kc	14.0 kc	7.1 kc	4.1 kc	1.7 kc	890 cps
1.0 "	112 "	32.9 "	14.0 "	7.1 "	4.1 "	1.7 "	890 "
10 "	112 "	32.9 "	14.0 "	7.1 "	4.1 "	1.7 "	890 "
100 "	112 "	32.9 "	14.0 "	7.1 "	4.1 "	1.7 "	890 "
1 kev	112 "	32.9 "	14.0 "	7.1 "	4.1 "	1.7 "	890 "
10 "	112 "	32.9 "	14.0 "	7.1 "	4.1 "	1.7 "	890 "
100 "	92.5 "	28.1 "	11.6 "	5.9 "	3.5 "	1.45 "	740 "
1 Mev	37.5 "	11.1 "	4.7 "	2.4 "	1.4 "	588 cps	300 "
10 "	4.8 "	1.4 "	0.6 "	0.3 "	177 cps	75 "	38 "

electrons at the high energy end is due to the increase in relativistic mass.

The Larmor frequencies of electrons in the energy range of interest are found to be of the order of from one kilocycle per second to several tens to kilocycles per second, which is well outside the frequency range for hydromagnetic disturbances. Thus, it appears that violation of the first invariant of electrons would require perturbations of other types which are outside the scope of this study. Effects of these types have been investigated by Parker (1961), Dungey (1963), and Cornwall (1964).

The Larmor frequencies of the protons of interest are of the order of one cycle per second to several tens of cycles per second. Since hydromagnetic waves propagate at frequencies less than the ion Larmor frequency, the possibility of violating the first invariant of protons with hydromagnetic disturbances does not seem to be good. Under conditions in which the wave crest and proton guiding center are moving along a line of force toward one another, it may be possible for the wave frequency to be Doppler shifted up to the proton Larmor frequency as viewed in a reference frame moving with the guiding center. This possibility has been investigated by Wentzel (1961a; 1961b; 1962), Dragt (1961), and Parker (1964).

B. Bounce Period

The bounce period T_m is defined as the length of time required for a trapped particle to travel from one mirror point to another and back again. Using this definition and assuming symmetry about the equatorial plane, we can write

$$T_m = 4 \int_{\theta_m}^{\pi/2} \frac{ds}{d\theta} \frac{d\theta}{v_{\parallel}(\theta)} \qquad (2.2)$$

where θ_m is the co-latitude of the mirror points, s is arc length measured along a line of force, and $v_{//}$ is the particle velocity component parallel to the field line. For our dipole field model the element of arc length is

$$ds = R_E L \sin\theta (1+3\cos^2\theta)^{\frac{1}{2}} d\theta \qquad (2.3)$$

where R_E is the radius of the earth and L is the distance in units of earth radii from the center of the earth to the field line in the geomagnetic equatorial plane. The dimensionless length L is equivalent to McIlwain's magnetic shell parameter for this model. Substitution of (2.3) into (2.2) gives

$$T_m = \frac{4 R_E L}{v} T(\mu) \qquad (2.4)$$

where

$$T(\mu) \equiv \int_{\theta_m(\mu)}^{\pi/2} \frac{\sin\theta (1+3\cos^2\theta)^{\frac{1}{2}}}{\left[1-\mu^2\left(\frac{1+3\cos^2\theta}{\sin^6\theta}\right)^{\frac{1}{2}}\right]^{\frac{1}{2}}} d\theta \qquad (2.5)$$

with $\mu = \sin\alpha$. This integral has been evaluated numerically by Hamlin (1961), who has shown that it can be approximated quite well by

$$T(\mu) \simeq 1.30 - 0.56\mu \qquad (2.6)$$

Values of T_m for both protons and electrons are given in Table II, where an equatorial pitch angle of 30° has been assumed. Since $T(\mu)$ changes by less than a factor of two over the entire range of pitch angles from zero to ninety degrees, the change in T_m over the same range is also less than a factor of two. If desired, the values of T_m for any pitch angle of α can be obtained by multiplying the values given in Table II by the factor $(1.27 - 0.55 \sin\alpha)$.

TABLE II

BOUNCE PERIODS

ENERGY \ L	2	3	4	5	6	8	10
Protons							
0.1 ev	197 min	292 min	395 min	498 min	595 min	790 min	1000 min
1.0 "	60 "	92 "	120 "	157 "	185 "	240 "	320 "
10 "	23 "	30 "	45 "	50 "	60 "	90 "	100 "
100 "	6.3 "	9.4 "	12.5 "	16 "	18.8 "	25 "	31 "
1 kev	2.0 "	3.0 "	4.0 "	300 sec	5.9 "	8 "	10 "
10 "	48 sec	1.0 "	1.4 "	94 "	2.0 "	2.8 "	3 "
100 "	12 "	18 sec	24 sec	30 "	36 sec	48 sec	60 sec
1 Mev	3.6 "	5.4 "	7.2 "	9 "	10.8 "	14.4 "	18 "
10 "	1.2 "	1.8 "	2.3 "	3 "	3.6 "	4.6 "	6 "
Electrons							
0.1 ev	4.7 min	6.9 min	9.4 min	11.6 min	13.8 min	18.8 min	23 min
1.0 "	1.4 "	2.2 "	2.8 "	3.7 "	4.3 "	5.6 "	7.4 "
10 "	29 sec	42 sec	58 sec	70 sec	84 sec	116 sec	140 sec
100 "	9 "	13 "	18 "	22 "	26 "	36 "	44 "
1 kev	2.8 "	4.3 "	5.7 "	7 "	8.5 "	11.4 "	14 "
10 "	0.8 "	1.2 "	1.5 "	2 "	2.3 "	3.0 "	4 "
100 "	0.3 "	0.4 "	0.6 "	0.7 "	0.8 "	1.2 "	1.4 "
1 Mev	0.08 "	0.1 "	0.2 "	0.2 "	0.2 "	0.3 "	0.4 "
10 "	0.03 "	0.04 "	0.06 "	0.07 "	0.08 "	0.1 "	0.1 "

Examination of Table II indicates that the bounce periods of electrons with energies greater than a kilovolt are less than 10 seconds. In particular, the bounce periods of electrons with energies of the order of a hundred kilovolts or greater are mostly less than one second. The situation for protons is somewhat different. Bounce periods for protons in an energy range from a few tens of kilovolts to 10 Mev range from the order of a minute down to about one second.

These calculations are presented graphically in Figure 2 (protons) and Figure 3 (electrons). The graphs allow estimates of the energies of the particles whose second invariants may be violated by a perturbation with a given period at a given L-value.

C. Drift Periods

The drift period of a trapped particle can be calculated by considering the instantaneous drift velocity of the guiding center as it moves in longitude, which can be written

$$v_\varphi = \frac{1}{\omega R}\left(v_{\parallel}^2 + 1/2\, v_\perp^2\right) \qquad (2.7)$$

where R is the local radius of curvature of the field line. In this expression only the field gradient and curvature drifts have been considered, which should be adequate for our purpose. Assuming symmetry about the equatorial plane, the change in the guiding-center longitude φ during one bounce period is

$$\Delta\varphi = 4\int_{\theta_m}^{\pi/2} \frac{ds}{d\theta}\,\frac{v_\varphi(\theta)\; d\theta}{v_{\parallel}(\theta)\, r(\theta)\, \sin\theta} \qquad (2.8)$$

Using the dipole field model, the average drift frequency is found to be

$$\Omega \equiv \frac{\Delta\varphi}{T_m} = \frac{3\gamma\, mc^3\, \beta^2}{eB_{eq}\, R_E^2\, L^2}\,\frac{E(\mu)}{T(\mu)} \qquad (2.9)$$

where B_{eq} is the field strength in the equatorial plane and $\beta \equiv \frac{v}{c}$. The function $E(\mu)$ is given by

$$E(\mu) = \int_{\theta_m(\mu)}^{\pi/2} \frac{\sin^3\theta\,(1+\cos^2\theta)}{(1+3\cos^2\theta)^{3/2}} \left[\frac{1+\mu^2\,\frac{(1+3\cos^2\theta)^{\frac{1}{2}}}{\sin^6\theta}}{1-\mu\,\frac{(1+3\cos^2\theta)^{\frac{1}{2}}}{\sin^6\theta}}\right]^{\frac{1}{2}} d\theta \quad (2.10)$$

This integral has also been evaluated by Hamlin (1961) who finds that a good approximation is

$$\frac{E(\mu)}{T(\mu)} \simeq 0.35 + 0.15\mu \quad (2.11)$$

The drift period is obtained using $T_d = 2\pi/\Omega$. Values of T_d calculated from (2.9) and (2.11) are given in Table III. An equatorial pitch angle of 30° was assumed in all cases. Drift periods for particles of arbitrary equatorial pitch angle α can be obtained by multiplying the values given in Table III by the factor $(0.82 + 0.35 \sin\alpha)$.

It is of interest to note that the drift decreases as L^{-1}. The drift periods for protons and electrons are approximately equal except at the higher energies where the change in relativistic mass ratio becomes significant for the electrons. In order to violate the third invariant of particles with energies greater than 100 kev, it appears that perturbations with a time scale from one to several tens of minutes are required. The calculations are presented in a graphical form in Figure 4.

D. Summary

Since hydromagnetic waves propagate at frequencies less than the local ion Larmor frequency, we would not expect to find hydromagnetic waves in the magnetosphere with frequencies higher

TABLE III

DRIFT PERIODS

ENERGY \ L	2	3	4	5	6	8	10
Protons							
0.1 ev	480 yrs	329 yrs	240 yrs	230 yrs	165 yrs	120 yrs	115 yrs
1.0 "	48 "	32.9 "	24 "	23 "	16.5 "	12 "	11.5 "
10 "	4.8 "	3.3 "	2.4 "	2.3 "	1.7 "	1.2 "	1.2 "
100 "	179 days	120 days	90 days	73 days	60 days	45 days	37 days
1 kev	17.9 "	12 "	9 "	175 hrs	6 "	4.5 "	88 hrs
10 "	43 hrs	28.8 hrs	22 hrs	17.5 "	14.4 hrs	11 hrs	8.7 "
100 "	262 min	173 min	131 min	105 min	86 min	65 min	52 min
1 Mev	26 "	17.3 "	13 "	600 sec	8.6 "	6.5 "	5 "
10 "	156 sec	104 sec	78 sec	60 "	52 sec	39 sec	30 sec
Electrons							
0.1 ev	480 yrs	329 yrs	240 yrs	230 yrs	165 yrs	120 yrs	115 yrs
1.0 "	48 "	32.9 "	24 "	23 "	16.5 "	12 "	11.5 "
10 "	4.8 "	3.3 "	2.4 "	2.3 "	1.7 "	1.2 "	1.2 "
100 "	179 days	120 days	90 days	73 days	60 days	45 days	37 days
1 kev	17.9 "	12 "	9 "	175 hrs	6 "	4.5 "	88 hrs
10 "	43 hrs	28.8 hrs	22 hrs	17.5 "	14.4 hrs	11 hrs	8.7 "
100 "	275 min	182 min	137 min	120 min	91 min	68 min	60 min
1 Mev	38 "	25.3 "	19 "	900 sec	12.7 "	9 "	450 sec
10 "	293 sec	195 sec	147 sec	105 "	97 sec	73 sec	52 "

than the Larmor frequencies for protons given in Table I. The electron Larmor frequencies are all considerably higher than the proton Larmor frequencies, so we would not expect violation of the first invariant of electrons by hydromagnetic waves. It may be possible for hydromagnetic waves propagating with frequencies near the local ion Larmor frequency to violate the first invariant of protons. If the wave and guiding center of the proton are moving toward one another, the wave will appear "Doppler shifted" to a higher frequency in the rest frame of the particle.

Reference to Table II indicates that hydromagnetic waves could violate the second invariant of both electrons and protons over essentially the entire range of energies and of L-values, except perhaps electrons at the highest energies considered at large L-values. Hydromagnetic waves with periods from about one second up to several tens of minutes should be effective in violating the second invariant of protons, while wave periods in the range from $\sim$ .05 second to 10 minutes should be capable of violating the second invariant of electrons.

The drift periods tabulated in Table III indicate that violation of the third invariant of both electrons and protons with energies greater than a few kev requires hydromagnetic waves with periods ranging from one minute to several hours.

CHAPTER III

VIOLATION OF THE SECOND INVARIANT BY SMALL-AMPLITUDE WAVES

A. Introduction

There exist a number of mechanisms which can produce violation of the second invariant, including the passage of compressional and transverse hydromagnetic waves across the mirror-point regions, the drift of mirror points into regions of rapidly changing field strength, and large-scale disturbances with rise times comparable to the particle bounce period. We shall now attempt to investigate quantitatively the effects produced in the particle motion when the second invariant is violated by small-amplitude magnetic disturbance. The passage of a wave across the mirror-point region of a particle causes a change in the total field strength, which in turn causes the mirror point to move along the field line. Since the particle will be reflected from a moving mirror point, Fermi acceleration can result. If a harmonic train of disturbances is present, the particle will make both headon and overtaking collisions with the mirror point, so that accelerations and decelerations of the particle will tend to cancel to first order, provided the waves are of sufficiently small amplitude. However, as we shall see in the following sections, a non-canceling second-order acceleration remains whenever the wave period and the particle periods are such that the second invariant is violated.

Before proceeding further, we need to establish a criterion for classifying a disturbance as "small amplitude". Let us consider a plot of field strength versus distance as we move along a field line as shown schematically in Figure 5. If the disturbance moves down the field line (toward increasing s), then particles with initial

mirror points such as that shown in the diagram can become trapped between the moving wave and a stationary mirror point and can undergo first-order Fermi acceleration which will continue until the particle develops enough energy to penetrate the wave. We see that first-order effects can occur only so long as the wave shows a pronounced peak on a B-versus-s plot. Kaufmann (1963) has pointed out that such peaks will cease to exist when $(dB/ds)_{wave} \sim dB_o/ds$ where B_o is the unperturbed field strength.

The quantity $(dB/ds)_{wave}$ can be estimated, using

$$\frac{dB}{ds}_{wave} \sim \frac{\Delta B}{t_r V_A} \qquad (3.1)$$

where ΔB is the amplitude of the wave, t_r is the rise time, and V_A is the Alfvén velocity. The derivative of the unperturbed field can be calculated, assuming the centered dipole field model used in Chapter II and using the expression (2.3) for the element of arc length ds, to obtain

$$\frac{dBo}{ds} = \frac{3.12 \times 10^{-6}}{L^4} \cdot \frac{3 \cos\theta \,(3 + 5 \cos^2\theta)}{\sin^8\theta \,(1 + 3 \cos^2\theta)} \quad \text{(gamma/earth radius)} \qquad (3.2)$$

Assuming that the condition $\frac{dB}{ds}_{wave} > \frac{dB_o}{ds}$ must be satisfied in order for first-order acceleration to occur, we can estimate the maximum mirror-point latitude $\lambda_m \left(= \frac{\pi}{2} - \theta_m \right)$ which a particle can have and still undergo first-order acceleration in the presence of a wave with a given amplitude and rise time. For a 10-gamma disturbance at L= 10, with a rise time of 10 seconds, assuming an Alfvén velocity of 500 km/sec, we find $(dB/ds)_{wave} \sim 13$ gamma/earth radius. From (3.2) the latitude at which $(dB/ds)_{wave} \sim dB_o/ds$ is found to be $\sim 20^o$. It is of interest to relate the mirror-point latitude to the equatorial

pitch angle of the particle. This can be done by assuming conservation of the first invariant which gives, for a dipole field

$$\sin^2 \alpha = \frac{B_{eq}}{B_m} = \frac{\cos^6 \lambda_m}{(1 + 3 \sin^2 \lambda_m)^{\frac{1}{2}}} \qquad (3.3)$$

where B_{eq} is the field strength at the equator and B_m is the field strength at the mirror point. A plot of λ_m versus α is given in Figure 6. The pitch angle corresponding to a mirror-point latitude of $\lambda_m = 20^\circ$ is $\alpha = 40^\circ$. Thus, in order for a particle to undergo first-order acceleration in the example considered above, it would have to have a pitch angle greater than 40°. At lower L-values the minimum pitch angle would increase. Hence, for disturbances with small amplitudes of the order of 10 gammas, we would expect first order acceleration to be confined to particles mirroring near the equatorial plane, with the effect being greatest at high L-values.

B. The Model

After having familiarized ourselves with some of the essential features of the problem, we would now like to proceed with a more quantitative investigation. However, before this can be done, a model must be chosen which will provide an adequate representation of the actual physical situation. Any attempt to use a dipole field as the unperturbed field results in equations of guiding-center motion which are not tractable, at least analytically. As a result it seems desirable to find a model of the unperturbed field which yields a less complicated guiding center equation, but which still preserves the essential features of a dipole-like field.

In an earlier study, Parker (1961) used an unperturbed field model of the form

$$B_o = B_{eq}(1 + \frac{s}{a}) \qquad (3.4)$$

where B_{eq} is the field strength at s = 0 (equatorial plane) and a is the characteristic length over which B_o varies. This model can be regarded as the first two terms in an expansion of the field or, somewhat more physically, it can be regarded as the field resulting from a dipole flux tube which has been bent out into a straight line. To complete the model, Parker chose to represent the hydromagnetic perturbation by a sinusoidal variation in the field strength, giving a total field of the form

$$B(s,t) = B_{eq}\left(1 + \frac{s}{a}\right) \left[1 + \mathcal{E} \sin (\omega t - \zeta)\right] \qquad (3.5)$$

where $\mathcal{E} = \Delta B/B_o$ and ζ is a phase factor used to relate the phase of the wave to the initial conditions of the particle motion.

The model should provide a reasonable representation of any mechanism which produces an approximate sinusoidal variation in the total field strength. In particular, the model probably best represents the propagation of compressional waves across field lines. Since this model seems to preserve the essential features of the physical situation and yields a tractable guiding center equation of motion, we shall adopt it also. In Parker's original analysis a restriction was imposed, such that only those particle energies and wave frequencies could be treated for which the condition $\omega T_m \lesssim 1$ was satisfied. We shall attempt to remove this restriction since, in general, there will be a considerable range of energies over which a wave of a given frequency will produce a significant effect, and we would like to be able to estimate this range. Alternatively, there will be a band of wave frequencies which will produce an appreciable effect on particles of a given energy.

C. Calculation of $\langle \Delta v_{\parallel} \rangle$ and $\langle (\Delta v_{\parallel})^2 \rangle$

The principal effect of the perturbation in the model which we have chosen is to produce a random walk of the particle mirror points down the field as the second order Fermi acceleration transfers energy from the perturbation into the parallel component of the particle motion. Thus, we have essentially two effects occurring; due to the migration of the particle mirror points down the field lines, the particles will eventually become lost into the atmosphere, but of those remaining in the trapping region at any given time, some will show an increase in energy.

In order to treat the problem quantitatively, the fundamental quantities to be calculated are the mean and mean square change per bounce period in the parallel component of particle velocity $v_{\parallel}$. To do this, we consider the motion of an individual particle starting with the guiding center equation, which in the absence of an electric field can be written

$$m \frac{d^2 s}{dt^2} = - \mu \frac{\partial B}{\partial s} \tag{3.6}$$

The use of this equation implies assumption of the conservation of the first invariant. Substitution of the field model (3.5) into (3.6) yields an equation of motion of the form

$$\frac{d^2 s}{dt^2} = - \frac{v_{o\perp}^2}{2a} \left[1 + \varepsilon \sin (\omega t - \delta) \right] \tag{3.7}$$

where we have used the relation for the diamagnetic moment $\mu = \frac{m v_{o\perp}^2}{2B_{eq}}$, with v_o being defined as the velocity of the particle at s = 0, at time t = 0.

The first integral of (3.7) gives the parallel component of the particle velocity

$$v_{\parallel} = v_{o_{\parallel}} - \frac{v_{o_\perp}^2}{2a} t + \frac{v_{o_\perp}^2 \mathcal{E}}{2a\omega} \left[\cos(\omega t - \zeta) - \cos\zeta\right] \quad (3.8)$$

and the second integral gives the position of the guiding center as a function of time

$$s = v_{o_{\parallel}} t - \frac{v_{o_\perp}^2}{4a} t^2 + \frac{v_{o_\perp}^2 \mathcal{E}}{2a\omega^2} \left[\sin(\omega t - \zeta) - \omega t \cos\zeta + \sin\zeta\right] \quad (3.9)$$

From these relations we would like to calculate the change in the particle's parallel velocity component when it returns to s = 0 after one bounce period. To do this, we must first calculate the time required for the particle to go from the origin to the mirror point and back to the origin again from (3.9) by letting s = 0 and solving for t. This value of t is then substituted into (3.7) to obtain the value of $v_{\parallel}$ when the particle returns to the origin.

Some practical difficulties are encountered in finding the roots of (3.9) with s set equal to zero, since it is transcendental to t. In order to solve this equation in Parker's analysis, an expansion of t in powers of ω was adopted, i.e.,

$$t = \sum_{n=0}^{\infty} f_n \omega^n \quad (3.10)$$

In order for this expansion to converge, it is necessary that $\omega t < 1$, which imposes the previously mentioned restriction. This restriction can be avoided if we choose $\mathcal{E}$ as an expansion parameter, and write

$$\omega t = a_0 + a_1 \mathcal{E} + a_2 \mathcal{E}^2 + \ldots. \quad (3.11)$$

Substitution of (3.11) into (3.9) with s set equal to zero yields an expression in ascending powers of $\mathcal{E}$. By setting the coefficient to each power of $\mathcal{E}$ separately equal to zero, we obtain a set of equations which can be solved for the coefficients a_0, a_1,

a_2, etc. In practice the calculations are carried out through order ε^2.

After finding the coefficients in (3.11), the resulting expression is substituted into (3.8) to give the change in the parallel velocity component during one bounce period $\Delta v_{o_{\parallel}}$. We now assume that all values of the phase δ of the wave relative to the initial condition of the particle are equally probable. This allows us to calculate the mean and mean square changes in $v_{o_{\parallel}}$ defined as

$$\langle \Delta v_{\parallel} \rangle \equiv \frac{1}{T_m} \cdot \frac{1}{2\pi} \int_0^{2\pi} \Delta v_{o_{\parallel}} \, d\delta \qquad (3.12)$$

and

$$\langle (\Delta v_{\parallel})^2 \rangle \equiv \frac{1}{T_m} \cdot \frac{1}{2\pi} \int_0^{2\pi} (\Delta v_{o_{\parallel}})^2 d\delta \qquad (3.13)$$

These and the preceding calculations require a large amount of straight-forward algebra, the details of which are given in Appendix A. The results of these calculations are

$$\langle \Delta v_{\parallel} \rangle = \frac{v_{o_\perp}^2 \varepsilon^2}{2a} \left[- \frac{\sin \omega T_m}{\omega T_m} + \frac{(1-3\cos\omega T_m)}{(\omega T_m)^2} + \frac{4 \sin \omega T_m}{(\omega T_m)^3} - \frac{4(1-\cos\omega T_m)}{(\omega T_m)^4} \right] + \theta(\varepsilon^3) \qquad (3.14)$$

and

$$\langle (\Delta v_{\parallel})^2 \rangle = \frac{v_{o_\perp}^2 \varepsilon^2}{4a^2 \omega} \left[\frac{(1+\cos\omega T_m)}{\omega T_m} - \frac{4 \sin \omega T_m}{(\omega T_m)^2} + \frac{4(1-\cos\omega T_m)}{(\omega T_m)^3} \right] + \theta(\varepsilon^3) \qquad (3.15)$$

If we expand (3.14) and (3.15) in powers of ωT_m and retain the lowest order non-vanishing term in each case, we obtain

$$\langle \Delta v_{\parallel} \rangle \approx \frac{v_{o\perp}^2 \varepsilon^2}{2a} \cdot \frac{5}{72} (\omega T_m)^2 \qquad (3.16)$$

and

$$\langle (\Delta v_{\parallel})^2 \rangle \approx \frac{v_{o\perp}^2 \varepsilon^2}{4a^2 \omega} \cdot \frac{1}{72} (\omega T_m)^3 \qquad (3.17)$$

These expressions are equivalent to the results obtained by Parker. Thus, our solution reduces to Parker's solution in the limit of small ωT_m as it should. Figures 7 and 8 show the behavior of $\langle \Delta v_{\parallel} \rangle$ and $\langle (\Delta v_{\parallel})^2 \rangle$, along with approximations (3.16) and (3.17).

The minima in $\langle (\Delta v_{\parallel})^2 \rangle$ and the zeroes in $\langle \Delta v_{\parallel} \rangle$ can be attributed to the existence of a perturbation along the entire length of the trajectory in the model which we are using. As a result, a particle can encounter perturbing accelerations which can tend to accelerate the particle along some parts of its trajectory and decelerate it along other parts. Because of this, cancellation can occur for certain ratios of the bounce period to the wave period. Cancellation can occur in two ways: the accelerations along the trajectory can cancel independent of the phase angle δ, or the changes produced in $\Delta v_{o\parallel}$ can be completely symmetrical in δ so that when the averaging over phase is carried out, cancellation occurs. The former accounts for the minima in $\langle (\Delta v_{\parallel})^2 \rangle$ and the zeroes near 3π, 5π, etc. in $\langle \Delta v_{\parallel} \rangle$, while the latter accounts for the zeroes in $\langle \Delta v_{\parallel} \rangle$ near 2π, 4π, etc.

The mean and mean square changes in the parallel component of velocity per bounce period provide good quantitative measures of the effectiveness of a disturbance of given frequency and amplitude in modifying particle motion. Examination of the $\langle (\Delta v_{o\parallel})^2 \rangle$ vs.

ωT_m curve indicates that the second invariant in this model is conserved only at certain discrete values of the ratio of the wave period to the particle bounce period. The maximum effect occurs when the wave and particle periods are of the same order, quantitatively confirming the usual statement, that for appreciable violation of the second invariant to occur, disturbances must be present with time scales comparable to the bounce period. The envelope of the curve falls off like $(\omega T_m)^{-1}$ for large ωT_m, as the large number of reversals of the perturbing acceleration during a bounce period tend to cancel more efficiently.

D. Mean Lifetimes and Diffusion Times

We would now like to use the expression for $\langle \Delta v_{\parallel} \rangle$ and $\langle (\Delta v_{\parallel})^2 \rangle$ derived in the previous section to calculate parameters which can be used in describing the physical behavior of a system of trapped particles in the presence of magnetic disturbances. It was pointed out earlier that as long as the first invariant is conserved, the component of particle motion transverse to the field line cannot undergo an irreversible acceleration. Hence, there can be no net change in $v_{o_\perp}$, the perpendicular component of particle velocity at the equator. Therefore, energy transferred from the wave to the particle motion will appear as an increase in the kinetic energy associated with the motion of the particle along the field line, i.e., $v_{o_\parallel}$ will change. When $v_{o_\parallel}$ increases while $v_{o_\perp}$ remains constant on the average, the equatorial pitch angle of the particle must decrease. As the pitch angle decreases, the particle's mirror point moves down the line of force. If the disturbance extends down to the atmosphere and persists over a sufficient period of time,

the mirror point will move into the dense atmosphere, and the particle will be removed from the trapping region through collisions with the air molecules.

Since evidence now exists that at least some hydromagnetic disturbances propagate from satellite altitudes to ground level (Patel, 1964), loss of trapped particles to the atmosphere can be expected to occur when such disturbances are present. It is of interest to calculate the change in energy which a particle can undergo before entering the atmosphere. If α_o is the initial equatorial pitch angle of the particle and α_c is the minimum equatorial pitch angle which a particle can have before entering the atmosphere, it follows directly from the conservation of the first invariant that the particle energy will be increased by the factor $\sin^2\alpha_o / \sin^2\alpha_c$. The cone centered on the field line at the equator with half-angle α_c is called the "loss cone." Any particle whose velocity vector at the equator lies within this cone will be lost to the atmosphere. If we let R_m be the geocentric distance to a mirror point, the latitude of the mirror point λ_m can be calculated, assuming a dipole field and using the equation for a field line.

$$R_m = R_e L \cos^2 \lambda_m \qquad (3.18)$$

Relation (3.3) can be used to relate α to λ_m. If we know the altitude at which atmospheric loss becomes important, (3.18) and (3.3) can be used to calculate α_c as a function of L. Since the altitude in question is of the order of hundreds of kilometers, for our purposes we can approximate this as the earth's surface. The values of α_c calculated in this way are shown in Figure 9. As an example of the sort of energy increase which can be expected before a particle becomes lost in the atmosphere, consider a particle with an equatorial

pitch angle of 30° at L = 4. From Figure 9 we see that $\alpha_c \approx 5^\circ$ so that energy is increased by a factor of $\sin^2 30^\circ / \sin^2 5^\circ \approx 33$.

In order to obtain some idea of the rate at which particles can become lost into the atmosphere, it is of interest to calculate characteristic lifetimes. To do this we begin by considering the diffusive and convective behavior of a system of noninteracting particles undergoing scattering in velocity space by some type of scattering agents. In our case velocity space is just a one-dimensional space defined by $v_{0_{\parallel}}$, and the scattering agents are the hydromagnetic waves. If we assume that there is no correlation between successive wave-particle encounters, then the random walk process can be treated, using the Fokker-Planck equation which in this case takes the form

$$\frac{\partial \psi}{\partial t} = \frac{1}{2} \frac{\partial^2}{\partial v_{0_{\parallel}}^2} \left[\langle (\Delta v_{\parallel})^2 \rangle \psi \right] - \frac{\partial}{\partial v_{0_{\parallel}}} \left[\langle \Delta v_{\parallel} \rangle \psi \right] \tag{3.19}$$

where $\psi(v_{0_{\parallel}}) dv_{0_{\parallel}}$ is the number of particles with velocities between $v_{0_{\parallel}}$ and $v_{0_{\parallel}} + dv_{0_{\parallel}}$. The derivation and properties of the Fokker-Planck equation are given in Appendix B. The assumption of no correlation between successive encounters is probably not completely valid for $\omega T_m < 1$, but (3.19) should still give essentially the correct results for sufficiently large values of the time t.

Let us now consider the solution of (3.19) for the case when $\langle (\Delta v_{\parallel})^2 \rangle$ and $\langle \Delta v_{\parallel} \rangle$ are constants. If we choose an initial distribution which is a delta function at some initial position $v_{0_{\parallel}} = u_0$, in the absence of boundaries we obtain (see Appendix B)

$$\psi(v_{o_{\parallel}}, t) \propto \exp\left\{ -\left[v_{o_{\parallel}} - (u_o + \langle \Delta v_{\parallel} \rangle t)\right]^2 \Big/ 2\langle (\Delta v_{\parallel})^2 \rangle t \right\} \tag{3.20}$$

This is a gaussian distribution moving toward increasing $v_{o_{\parallel}}$, instantaneously centered at $v_{o_{\parallel}} = u_o + \langle \Delta v_{\parallel} \rangle t$ with an instantaneous half-width $\sqrt{2\langle (\Delta v_{\parallel})^2 \rangle t}$. From this we see that $\langle \Delta v_{\parallel} \rangle$ is a measure of the convective motion of the particles in velocity space and $\langle (\Delta v_{\parallel})^2 \rangle$ is a measure of the spread in the distribution, or the diffusion.

In the case we are considering, particles with an initial parallel component of velocity u_o can undergo an increase in velocity up to some value of u_c at which point the particles become lost from the trapping region. This suggests defining a characteristic lifetime of the form

$$\tau_L \equiv \frac{u_c - u_o}{\langle \Delta v_{\parallel} \rangle} \tag{3.21}$$

This definition is not entirely satisfactory as it stands, however. In the analysis above it was assumed that $\langle \Delta v_{\parallel} \rangle$ and $\langle (\Delta v_{\parallel})^2 \rangle$ were constants. In the case we are considering, they are not constant but depend on $v_{o_{\parallel}}$ through T_m. The most obvious modification to (3.21) is to replace $\langle \Delta v_{\parallel} \rangle$ by its mean value between the two limits of ωT_m corresponding to $v_{o_{\parallel}} = u_o$ and $v_{o_{\parallel}} = u_c$, i.e.,

$$\overline{\langle \Delta v_{\parallel} \rangle} \equiv \frac{1}{|x_o - x_c|} \int_{x_o}^{x_c} \langle \Delta v_{\parallel} \rangle \, dx \tag{3.22}$$

where we have let $x = \omega T_m$. The definition of the characteristic lifetime is now modified to read

$$\tau_L \equiv \frac{u_c - u_o}{\overline{\langle \Delta v_{\parallel} \rangle}} \tag{3.23}$$

Using (3.14) we can carry out the integration in (3.22) to obtain

the distribution will be of the form

$$\psi(v_{o_{\parallel}}, t) = \frac{N_o}{\sqrt{\pi}} \left[2 \langle (\Delta v_{\parallel})^2 \rangle t \right]^{-\frac{1}{2}} \exp \left[-(v_{o_{\parallel}} - u_1)^2 / 2 \langle (\Delta v_{\parallel})^2 \rangle t \right] \tag{3.29}$$

where N_o is the total number of particles and u_1 is the mid-point of the interval between u_o and u_c. Evidently, the half-width of the gaussian distribution at the 1/e point at time t is $\sqrt{2 \langle (\Delta v_{\parallel})^2 \rangle t}$. The ratio of the total width of the distribution to the interval between u_o and u_c is

$$Y = \frac{2\sqrt{2 \langle (\Delta v_{\parallel})^2 \rangle t}}{u_c - u_o} \tag{3.30}$$

A characteristic diffusion time τ_D can be defined as the time required for this ratio to assume some arbitrarily chosen value. When this ratio is established, τ_D is obtained from (3.30) in the form

$$\tau_D = \frac{Y^2 u_o^2 (\frac{u_c}{u_o} - 1)^2}{8 \overline{\langle (\Delta v_{\parallel})^2 \rangle}} \tag{3.31}$$

where we have replaced $\langle (\Delta v_{\parallel})^2 \rangle$ by its mean value which can be written (Appendix C)

$$\overline{\langle (\Delta v_{\parallel})^2 \rangle} = \frac{4 u_o^2 \omega \varepsilon^2}{x_o^2} \cdot \frac{G(x_o) - G(x_c)}{x_o - x_c} \tag{3.32}$$

The function G(x) is defined as

$$G(x) = \ell n(\gamma x) - 1 - Ci(x) + \frac{2 \sin x}{x} - \frac{2(1-\cos x)}{x^2} \tag{3.33}$$

where $\ell n \gamma$ is the Euler's constant (= 0.577...) and Ci(x) is the Integral Cosine Function (Jahnke and Emde, 1945). Combining (3.32) and (3.33) we finally obtain

$$\tau_D = \frac{Y^2}{8} \left(\frac{\tan\alpha_o}{\tan\alpha_c} - 1\right)^2 \left(1 - \frac{x_c}{x_o}\right) \frac{x_o^2}{4\xi^2 \left[G(x_o) - G(x_c)\right]} T_m^{(o)} \tag{3.34}$$

It should be noted that in arriving at relations (3.27) and (3.34), we have tacitly assumed that the expressions for $\langle \Delta v_{\parallel} \rangle / v_{\parallel}$ and $\langle (\Delta v_{\parallel})^2 \rangle / v_{\parallel}^2$ as functions to T_m obtained from the model are reasonable approximations to what would be obtained from the actual magnetosphere. The behavior of the wave amplitude as a function of distance along a field line is somewhat unrealistic in the model. The requirement that the ratio of the wave amplitude to the unperturbed field strength be a constant implies an increasing amplitude as we move down a field line, while a decreasing amplitude probably would be more realistic. The field lines of the model do not converge as rapidly as the lines of a dipole field. For this reason the dependence of the bounce period on the parallel component of particle velocity is not the same. However, the model does contain the essential features of the converging field lines of the mirror geometry found in the magnetosphere, with the mirror point set in motion by a changing field strength in the mirror point region. For this reason it is felt that (3.27) and (3.34) provide reasonable estimates of the characteristic times involved in the process.

Both τ_L and τ_D depend in general on the particle energy, pitch angle, L-value, and on the wave period and amplitude. As an example which may be of some interest, calculated values of τ_L versus particle energy for protons at L = 4 with an initial pitch angle of 30° in the presence of disturbances of 10-gammas amplitude at the initial mirror point are shown in Figure 10. Wave periods from 10 seconds to 100 seconds are included. Similar calculations for electrons are shown in Figure 11 for wave periods of from 1 sec-

ond to 10 seconds. Examples of characteristic diffusion times are given in Figure 12 for protons at L = 4, $\alpha_o = 30^o$, and for a wave of 100-second period and 10-gamma amplitude. Calculations have been made, using as a criterion a spread in the distribution such that the full width of the distribution is equal to $u_c - u_o$ (Y = 1 in (3.31)). The corresponding curve of τ_L is shown for comparison purposes. In order to obtain some idea of how τ_L varies with changing L-value, calculations were made for protons at L = 8 and a wave period of 50 seconds with an amplitude of 10 gammas at the initial mirror points. These calculations along with the corresponding values at L = 4 are shown in Figure 13.

The sample calculations indicate that for a given wave period, the maximum disturbance occurs for particles in an energy band approximately two decades wide. Examination of Figure 10 gives some feeling for the dependence of the characteristic lifetimes on the wave period. As we proceed toward shorter periods, the minimum in the τ_L versus energy curve shifts toward higher energies and the magnitude of τ_L decreases. In the example considered, for a wave period of 100 seconds, the characteristic lifetimes are of the order of 500 days in an energy band from 5 kev to 500 kev, while for a wave period of 10 seconds the characteristic lifetimes are down to the order of 50 days, and the energy band in which the maximum effect occurs has shifted up to an interval between 500 kev and 50 Mev. The calculations for electrons shown in Figure 11 indicate that in order to reach the energy range from tens of kilovolts to several Mev it is necessary to go to wave periods about an order of magnitude smaller than in the case of protons.

From the comparison of τ_D and τ_L shown in Figure 12, we see that τ_D is of the same order of magnitude as τ_L. This indicates a considerable spread in the distribution function can be expected to occur in times of the order of τ_L. This effect is manifested in a spreading out along the lines of force of the mirror points of particles having the same initial pitch angle. Thus, short diffusion times indicate that the distribution of particles at a given time is not strongly dependent on the particle source mechanism, since any structure in the distribution is rapidly smoothed out.

From Figure 13 we obtain some idea of the way in which τ_L changes with increasing L-value. The values of τ_L decrease by about an order of magnitude in going from L = 4 to L = 8, which illustrates the relatively greater stability against magnetic disturbances of the particles at lower L-values. The relatively short characteristic lifetimes of the order of tens of days at L = 8 indicate that if disturbances of periods of the order of tens of seconds exist during a reasonable percentage of the time, they could play a role in defining the outer limits of the proton distribution in the magnetosphere. The shorter period disturbances would tend to affect the high energy end of the proton distribution, softening the spectrum at higher L-values.

From (3.27) and (3.34) we see that the characteristic times are inversely proportional to the square of the relative wave amplitude. The calculations discussed above are all based on a 10-gamma amplitude. A one-gamma amplitude would result in a characteristic lifetime one hundred times longer than those given above.

E. Summary

Estimates of characteristic lifetimes and characteristic dif-

fusion times have been made using a model originally employed by Parker (1961). In the original analysis the restriction $\omega T_m < 1$ was imposed. In the present analysis this restriction has been removed, allowing an estimate to be made of the particle energy band over which a wave of a given period produces a significant effect. Sample calculations of characteristic lifetimes versus particle energy indicate that the effects of a monochromatic wave are felt by particles in an energy band approximately two decades wide, with the high energy end corresponding to the energy for which $\omega T_m \sim 1$.

Characteristic diffusion times are found to be of the same order as the characteristic lifetimes, indicating the importance of the diffusive behavior of the particles. For a group of particles initially having the same mirror point, an appreciable spread in mirror points can be expected to develop as they execute a random walk down the field line.

Calculations of proton characteristic lifetimes for L = 4 and L = 8 indicate that the energy band of particles affected by a disturbance shifts toward higher energies with increasing L-value, while the characteristic lifetimes decrease. If hydromagnetic disturbances are present in sufficient abundance with periods of the order of tens of seconds, they could play a role in the dynamics of the outer part of the region of trapped protons. The tendency of the shorter period waves to affect the higher energy particles could produce a steepening of the energy spectrum toward higher L-values.

Sample calculations of characteristic lifetimes for electrons at L = 4 indicate that in order for electrons in the 10 kev to several Mev energy range to be affected, waves with periods from 10 seconds down to one second would be necessary.

CHAPTER IV

VIOLATION OF THE THIRD INVARIANT BY LARGE-SCALE MAGNETIC DISTURBANCES

We shall now consider magnetic disturbances which can violate the third or flux invariant of the particle motion. Mechanisms capable of producing such a violation include magnetic storm sudden commencements, sudden impulses, sinusoidal magnetospheric boundary motion, convective systems within the magnetosphere, transverse waves with periods near the drift period, localized long period disturbances, and long period compressional waves not associated with boundary motion (such as those generated by exospheric gravity waves (Patel, 1965)). In order for such violations to occur, it is necessary for the disturbances to have time scales comparable to the particle drift period. The principal effect is to produce a diffusion of particles across magnetic shells. We shall consider only disturbances of sufficiently large scale to extend over the entire trajectory of the particle as it drifts in longitude.

A. Models for Large-Scale Magnetic Disturbances

The first attempt at a quantitative treatment of the violation of the third invariant by magnetic disturbances was made by Parker (1960), although Herlofson (1960) had previously considered the diffusion of particles across magnetic shells without considering specific models. In Parker's study the unperturbed

field is assumed to be a dipole. A magnetic storm type of disturbance, based on the Chapman-Ferraro model, is simulated by bringing a conducting plane oriented parallel to the dipole axis up from infinity in a time very short compared to the drift period of the particles. The plane is then held in place for a time comparable to the drift period or longer, and finally withdrawn either abruptly or slowly. Only particles mirroring at the equator are considered.

The physical picture of what happens to the particles when such a disturbance occurs is easy to follow qualitatively. Consider a ring of particles drifting in the equatorial plane of the dipole field. The particles will drift along a contour of constant field strength which will be a circle in the unperturbed field. When the conducting plane is brought up, the field will tend to be compressed. If this is done very rapidly compared to the particle drift period, the particle will remain essentially on the same field line and move with the thermal plasma and the field line. Viewed in another way, the plane must be brought up so rapidly that the drift velocity $\underline{v}_E$ due to the induced E-field is much greater than the gradient drift velocity $\underline{v}_G$. When the field is compressed, the ring of particles is suddenly displaced in a direction away from the plane and is no longer centered on the dipole. If the plane is then held in place for a time long compared to the drift period, each particle in the initial ring will drift along a new contour of constant field strength. Since the centers of the new contours of constant field strength are shifted off the dipole in the direction of the conducting plane, and the center of the initial ring is displaced in the opposite

direction, the particles will no longer all drift along a common contour. Each particle will move along a slightly different contour. If the plane is now withdrawn slowly, the new contours will become recentered on the dipole, and the particles which were initially in a ring will now be spread out into a band. Particles with the same initial L-value will be distributed over a range of L-values.

In Parker's analysis the mean square change per disturbance in the geocentric distance of the particles was calculated, and their diffusive behavior was investigated, using an heuristically derived diffusion equation. This analysis was later modified by Davis and Chang (1962) who derived both the mean and mean square changes in the radial distance and used the Fokker-Planck formulation to treat the diffusion.

This model is probably reasonably well suited for the treatment of magnetic storm sudden commencement type perturbations, which was the original intent of both Parker and Davis and Chang. It may also be applicable to the sudden impulse disturbances which are observed both at satellite altitudes and on a worldwide basis on the ground (Nishida, 1963; Nishida and Cahill, 1964). Such an application is now being pursued by Hess and his colleagues (Hess, 1965).

In Parker's model the perturbed field can be calculated when the plane has been moved in to a distance ℓ from the dipole by placing an image dipole of the same strength a distance 2ℓ away. When this is done, the perturbed field is found to be given approximately by (Parker, 1960)

$$
\left.
\begin{aligned}
B_R &= \frac{2M}{R^3}\cos\theta + \frac{M}{8\ell^3}\left[-\cos\theta + \frac{3R}{2\ell}\sin 2\theta \sin\bar{\phi}\right] \\
B_\theta &= \frac{M}{R^3}\sin\theta + \frac{M}{8\ell^3}\left[\sin\theta + \frac{3R}{2\ell}\cos 2\theta \sin\bar{\phi}\right] \\
B_{\bar{\phi}} &= \frac{3MR}{16\ell^4}\cos\theta\cos\bar{\phi}
\end{aligned}
\right\} \quad (4.1)
$$

where M is the magnetic dipole moment and the coordinates R, θ, and $\bar{\phi}$ are the spherical polar coordinates defined in Figure 14. Expressions (4.1) are valid only for values of R somewhat less than ℓ. The first terms in B_R and B_θ are simply the contributions of the unperturbed dipole field and the remaining terms represent the perturbation field. Using the sudden disturbance model and (4.1), Davis and Chang were able to calculate the mean and mean square displacement per disturbance of the radial distance of the particles by considering the displacement of the field lines and assuming the particles remained on the field lines during the displacement. Their results for the lowest non-vanishing order in R/ℓ are

$$
\left.
\begin{aligned}
\langle \Delta R \rangle &= 2\left(\frac{15}{112}\right)^2 R\left(\frac{R}{\ell}\right)^4 \\
\langle (\Delta R)^2 \rangle &= \frac{1}{2}\left(\frac{15}{112}\right)^2 R^2\left(\frac{R}{\ell}\right)^8
\end{aligned}
\right\} \quad (4.2)
$$

We see that both quantities increase rather rapidly with increasing radial distance. Physically, this means that particles moving inward will tend to diffuse more slowly, while the rate of diffusion for particles moving outward will increase. As a distribution which is initially a delta function spreads out, particles near the inner edge are depleted more slowly than those near the outer edge. As a result, the distribution becomes distorted with a steep

inner edge, giving the appearance of a wave with its crest moving inward. The position of this crest is found by Davis and Chang to be given approximately by

$$\left(\frac{Rc}{\ell}\right)^8 = \frac{1}{14}\left(\frac{15}{112}\right)^{-2} n^{-1} \qquad (4.3)$$

where Rc is the position of the wave crest and n is the number of disturbances which have occurred. This is an asymptotic form good for large n. From (4.3) we find that the apparent inward velocity of the crest is

$$\frac{dR_c}{dt} = -\frac{7}{4}\left(\frac{15}{112}\right)^2 R_c \left(\frac{R_c}{\ell}\right)^8 \frac{dn}{dt} \qquad (4.4)$$

where dn/dt is the number of disturbances occurring per unit time.

B. Calculation of $\langle(\Delta R)^2\rangle$ for a Sinusoidal Disturbance

It is of interest to consider the possibility of performing an analysis similar to that discussed in the previous section without requiring a sudden rise time, since such a non-linear treatment requires a perturbation of a rather special shape. In particular we would like to be able to treat a disturbance with a sinusoidal behavior. If we consider modifications of (4.1) such that the perturbation field has a sinusoidal time dependence with a frequency ω, the most obvious modification which is linear in $\sin \omega t$ is

$$\left.\begin{aligned} B_R &= \frac{2M}{R^3}\cos\Theta + \frac{M}{8\ell^3}\left[-\cos\Theta + \frac{3R}{2\ell}\sin 2\Theta \sin\Phi\right]\sin\omega t \\ B_\Theta &= \frac{M}{R^3}\sin\Theta + \frac{M}{8\ell^3}\left[\sin\Theta + \frac{3R}{2\ell}\cos 2\Theta \sin\Phi\right]\sin\omega t \\ B_\Phi &= \frac{3MR}{16\ell^4}\cos\Theta\cos\Phi\sin\omega t \end{aligned}\right\} \qquad (4.5)$$

We shall adopt this as our model. Violation of the third invariant by sinusoidal boundary motion should be well represented by this model, as should any large-scale compressional disturbances propagating in the equatorial plane.

In order to calculate the mean square change in the particle geocentric distance per disturbance cycle, it is necessary to first consider the drift behavior of individual particles. The drift velocity of a particle mirroring in the equatorial plane is composed of the sum of two parts: the gradient drift

$$\underline{v}_G = \frac{mc v^2}{2eB} \frac{\underline{B} \times \nabla_\perp B}{B^2} \tag{4.6}$$

and the E x B drift due to the induced E-Field

$$\underline{v}_E = \frac{\underline{E} \times \underline{B}}{B^2} c \tag{4.7}$$

In the analysis of Parker and of Davis and Chang in which $v_G << v_E$ during the initial part of the perturbation, ΔR could be found by calculating the displacement of the field lines on which the particles are trapped. In our case v_G and v_E may be of the same order throughout the perturbation, so explicit expressions for $\underline{v}_G$ and $\underline{v}_E$ are needed.

In general, the calculation of the induced E-field is rather difficult. However, in the model we are considering in which the $\underline{B}$-field is completely specified at each point at all times, knowledge of an explicit expression for $\underline{E}$ is unnecessary. The value of $\underline{v}_E$ will be the same for both the thermal plasma in the magnetosphere and the energetic particles, since (4.7) is independent of particle parameters. However, the gradient drift (4.6) is proportional to the particle energy, so the relatively

low energy plasma will have drift periods of the order of years (cf. Table III). Since we are considering time scales of the order of tens of minutes, the plasma motion will be determined by $\underline{v}_E$. Since the field can be assumed to be frozen in the plasma, the plasma motion in the equatorial plane and hence $\underline{v}_E$ can be deduced by following the motion of the points of intersection of the field lines with the equatorial plane.

The equations for a line of force can be obtained from the defining relations

$$\frac{dR}{B_R} = \frac{R d\theta}{B_\theta} = \frac{R \sin\theta}{B_\theta} d\bar{\Phi} \qquad (4.8)$$

Substitution of (4.5) into (4.8) with the retension of terms through order $(R/\ell)^4$ gives

$$\frac{1}{R}\frac{dR}{d} = 2\frac{\cos}{\sin\theta} - \frac{3R^3}{8\ell^3}\frac{\cos\theta}{\sin\theta}\left[1 + \frac{R}{\ell}\frac{\sin\bar{\Phi}}{\sin\theta}(1-\bar{3}\sin^2\theta)\right]\sin\omega t$$
$$\frac{d\bar{\Phi}}{d\theta} = \frac{3R^4}{16\ell^4}\frac{\cos\theta\cos\bar{\Phi}}{\sin^2\theta}\sin\omega t \qquad (4.9)$$

This is a set of coupled first order differential equations, for which the solutions $R(\theta;t)$ and $\bar{\Phi}(\theta;t)$ represent a line of force at some instant of time. These must be solved by successive approximation. We do this by noting that in the absence of the perturbation ($\ell \to \infty$), equations (4.9) have the solution

$$R = r\sin^2\theta$$
$$\bar{\Phi} = \varphi \qquad (4.10)$$

where r and φ are constants of integration. These are just the equations of the unperturbed dipole field which intersects the equatorial plane at $R = r$ and $\bar{\Phi} = \varphi$. Taking (4.10) as a

first approximation and substituting these values into the right-hand side of (4.9), the integration can be carried out to give a second approximation. The result with Θ set equal to $\pi/2$ is

$$\left.\begin{aligned} R &= r\left[1 - \frac{3r^3}{8\ell^3}\left(\frac{1}{6} - \frac{4}{21}\frac{r}{\ell}\sin\varphi\right)\sin\omega t\right] \\ \Phi &= \varphi + \frac{3r^4}{112\ell^4}\cos\varphi\sin\omega t \end{aligned}\right\} \quad (4.11)$$

This defines the intersection with the equatorial plane of a field line at time t whose point of intersection in the absence of the perturbation is $R = r$, $\Phi = \varphi$. We can use the parameters r and φ to "label" a particular field line and follow its motion in the equatorial plane as a function of time, using (4.11).

Now the velocity of the point of intersection with the equatorial plane of a field labeled r, φ at time t is obtained by taking the time derivative of R and Φ. The result is

$$\left.\begin{aligned} \frac{dR}{dt} &= -r\omega\left[\frac{3r^3}{8\ell^3}\left(\frac{1}{6} - \frac{4}{21}\frac{r}{\ell}\sin\varphi\right)\right]\cos\omega t \\ R\frac{d\Phi}{dt} &= r\omega\left[\frac{3r^4}{112\ell^4}\cos\varphi\right]\cos\omega t \end{aligned}\right\} \quad (4.12)$$

The velocity of the thermal plasma at the point (R, Φ) in the equatorial plane at time t is just the velocity of the line which is located at (R, Φ) at time t. The label of the line at (R, Φ) at time t is determined by inverting equations (4.11) to obtain r and φ in the form

$$\left.\begin{aligned} r &= r\,(R, \Phi ; t) \\ \varphi &= \varphi\,(R, \Phi ; t) \end{aligned}\right\} \qquad (4.13)$$

The values of r and φ obtained in this way are substituted into (4.12) to obtain the components of $\underline{v}_E$ in the equatorial plane in the form

$$\left.\begin{aligned} v_{ER} &= -\omega R \left[\frac{3R^3}{8\ell^3}\left(\frac{1}{6} - \frac{4}{21}\frac{R}{\ell}\sin\Phi\right)\right] \cos\omega t \\ v_{E\Phi} &= \omega R \left[\frac{3R^4}{112\ell^4}\cos\Phi\right] \cos\omega t \end{aligned}\right\} \qquad (4.14)$$

It is helpful to attempt to picture the behavior of the magnetic field at the equatorial plane as it is subjected to the perturbation. Consider the set of field lines intersecting the equatorial plane along the circle of radius r centered on the dipole at time $t = 0$, as shown in Figure 15. The points of intersection of these lines will oscillate between the limits indicated by the broken contours. (The amplitude of this motion is exaggerated in the drawing.) The trajectories of several of the intersection points are shown. The lowest order change in the contour is a shift of order r^4/ℓ^4 of the center of the circle along the line joining the dipoles and a change in its radius of order r^3/ℓ^3.

We must now calculate the drift velocity. It is convenient to rewrite (4.6) in the form

$$\underline{v}_G = \frac{c\mu}{e}\hat{\Theta} \times \frac{\nabla_\perp B}{B} \qquad (4.15)$$

where $\hat{\Theta}$ is a unit vector normal to the equatorial plane and μ

is the first invariant, which we assume is conserved throughout the perturbation. Using (4.5) and (4.15) we obtain $\underline{v}_G$ which, written in component form, is

$$v_{GR} = -\frac{3c\mu}{e} \cdot \frac{1}{R} \left[\frac{R^4}{16\ell^4} \cos \Phi \right] \sin \omega t \tag{4.16}$$

$$v_{G\Phi} = \frac{3c\mu}{e} \cdot \frac{1}{R} \left[1 - \frac{R^3}{8\ell^3} \left(1-2\frac{R}{\ell} \sin \Phi \right) \sin \omega t \right]$$

The total drift velocity is obtained by adding (4.14) and (4.16), giving the guiding center equations of the particle motion

$$\frac{dR}{dt} = -\omega R \left[\frac{3R^3}{8\ell^3} \left(\frac{1}{6} - \frac{4}{21} \frac{R}{\ell} \sin \Phi \right) \cos \omega t \right]$$

$$R \frac{d\Phi}{dt} = \omega R \frac{3R^4}{112\ell^4} \cos \Phi \cos \omega t \tag{4.17}$$

$$+ \frac{3c\mu}{e} \cdot \frac{1}{R} \left[1 - \frac{R^3}{8\ell^3} \left(1-2\frac{R}{\ell} \sin \Phi \right) \sin \omega t \right]$$

We would like to obtain R(t). To do this we must resort to successive approximation once again. In the absence of the perturbation, the solution to (4.17) is

$$\left.\begin{aligned} R &= R_o \\ \Phi &= \Phi_o + \Omega t \end{aligned}\right\} \tag{4.18}$$

where R_o and Φ_o are constants of integration, and Ω is the angular drift frequency

$$\Omega = \frac{3c\mu}{eR_o^2} \tag{4.19}$$

Taking (4.18) as a first approximation and substituting into the

right-hand side of (4.17), the equations of motion can be integrated to give a second approximation. The result for R(t) is

$$R(t) = R_o \left\{ 1 - \frac{R_o^3}{16\ell^3} \sin \omega t + \omega \frac{R_o^4}{14\ell^4} \left[\sin \Phi_o \frac{\sin(\Omega-\omega)t}{2(\Omega-\omega)} + \frac{\sin(\Omega+\omega)t}{2(\Omega+\omega)} + \cos \Phi_o \left(\frac{1-\cos(\Omega-\omega)t}{2(\Omega-\omega)} + \frac{1-\cos(\Omega+\omega)t}{2(\Omega+\omega)} \right) \right] \right.$$
$$\left. - \Omega \frac{R_o^4}{16\ell^4} \left[\cos \Phi_o \left(\frac{\cos(\Omega-\omega)t-1}{2(\Omega-\omega)} - \frac{\cos(\Omega+\omega)t-1}{2(\Omega+\omega)} \right) + \sin \Phi_o \left(\frac{\sin(\Omega-\omega)t}{2(\Omega-\omega)} - \frac{\sin(\Omega+\omega)t}{2(\Omega+\omega)} \right) \right] \right\} \tag{4.20}$$

The constant of integration has been chosen such that $R = R_o$ when $t = 0$. Note that the higher order terms in (4.20) show the characteristics of resonance behavior for $\omega = \Omega$.

The change in R during one disturbance cycle can be calculated from (4.20) by letting $t = 2\pi/\omega$. This gives

$$\Delta R = \frac{15}{112} R_o \frac{R_o^4}{\ell^4} \frac{\omega\Omega}{(\Omega^2-\omega^2)} \left[\sin \Phi_o \sin\left(2\pi\frac{\Omega}{\omega}\right) - \cos \Phi_o \left(\cos 2\pi\frac{\Omega}{\omega} - 1\right) \right] + \mathcal{O}\left(\frac{R^5}{\ell^5}\right) \tag{4.21}$$

If we assume that all initial position angles Φ_o of the particle are equally probable, we can perform an average over Φ_o. Squaring (4.21) and carrying out the averaging, we obtain

$$\langle (\Delta R)^2 \rangle = \left(\frac{15}{112}\right)^2 R_o^2 \left(\frac{R_o}{\ell}\right)^8 \frac{\left(\frac{\Omega}{\omega}\right)^2}{\left[\left(\frac{\Omega}{\omega}\right)^2 - 1\right]^2} \left[1 - \cos\left(2\pi\frac{\Omega}{\omega}\right)\right] \tag{4.22}$$

This is the desired result for the mean square change in radial

position per disturbance cycle.

The dependence of $\langle (\Delta R)^2 \rangle$ on the disturbance frequency is shown in Figure 16. The resonance-like behavior is due to the fact that the particles are subjected to a perturbation throughout their entire trajectory. Maximum changes occur in R when the drift period and the period of the perturbation are approximately equal. When the perturbation period is an integral multiple of the drift period greater than or equal to two, the effect of the perturbation is completely canceled out over one period and nulls in $\langle (\Delta R)^2 \rangle$ are obtained. At large values of the perturbation period, the third invariant is no longer violated appreciably.

Comparing (4.22) with the result obtained from the sudden disturbance model (4.2), we see that the sinusoidal model modifies $\langle (\Delta R)^2 \rangle$ by a factor of twice the frequency dependent function shown in Figure 16. Thus, for values of R where the resonance effect is strongest ($\Omega \approx \omega$) the value of $\langle (\Delta R)^2 \rangle$ for a sinusoidal disturbance can be about ten times as large as that for a sudden disturbance of the same amplitude. For other values of R, where the sinusoidal disturbance is off resonance, the sinusoidal value of $\langle (\Delta R)^2 \rangle$ can be much smaller. Thus, for this mechanism to be most effective, it is necessary that waves with periods within a few minutes of the particle drift period be present a substantial fraction of the time. There is some evidence that certain types of waves may propagate most frequently near a particular period (Patel, 1965), but this is based on a very small sampling of data. In order to ascertain if such a condition occurs regularly in the magnetosphere, much more

extensive studies will have to be carried out.

C. Calculation of Diffusion Times

We would now like to calculate characteristic diffusion times from the expression for $\langle (\Delta R)^2 \rangle$ obtained in the previous section. To do this, we once again consider the solution of the Fokker-Planck equation with constant diffusion coefficients (Appendix C). In this case we are considering a distribution in a one-dimensional space defined by the radial distance R. Consider a δ-function distribution at time t = 0 at some particular value of R. The half-width of the distribution a at time t is then given by

$$a^2 = 2 \langle (\Delta R)^2 \rangle \quad t \tag{4.23}$$

We can now define a diffusion time t_D as the time required for the distribution to spread to some arbitrary half-width a_1. This can be written

$$t_D \equiv \frac{a_1^2}{2 \langle (\Delta R)^2 \rangle} \tag{4.24}$$

The diffusion time provides a characteristic time scale over which the diffusion proceeds at a given radial distance, neglecting the convective part of the motion.

The diffusion time defined by (4.24) will depend in general on the radial distance and the magnetic moment of the particles being considered. The dependence on magnetic moment results from the assumption that the first invariant is conserved during the diffusion process. The energy of the particles changes

as they move from one shell to another, going as L^{-3} for non-relativistic particles.

As an example we shall consider a particular case for which the diffusive behavior of particles is of considerable interest. An apparent radial diffusion of electrons with energies greater than 1.6 Mev has been observed in Explorer 14 by Frank, Van Allen and Hills (1964) and by Frank (1965). Under post-magnetic storm conditions, an apparent inward motion of a "wave" of electrons was observed between L = 4.8 and L = 3.4. The apparent inward velocity of the wave was $\sim$ 0.4 R_E /day at L = 4.8, decreasing to $\sim$ 0.03 R_E /day at L = 3.4. To investigate the diffusive behavior which the model we are considering would predict in this region, characteristic diffusion times were calculated for electrons which would have an energy of 1.6 Mev at L = 4. A value of ℓ = 11.3 earth radii was used, which corresponds to a perturbation of 10-gamma amplitude at L = 8 along the earth-sun line and approximately 5 γ at L = 4. The results of the calculations for disturbance periods of 5, 10 and 20 minutes are shown in Figure 17. The value of α_1 in (4.24) was taken as one earth radius. For 1.6 Mev electron at L = 4, the drift period is 12.8 minutes. In the same figure the diffusion time obtained from the value of $\langle (\Delta R)^2 \rangle$ which is obtained from the Davis and Chang model is shown. In this model the diffusion time is proportional to the quotient $\ell^8 / \frac{dn}{dt}$, where $\frac{dn}{dt}$ is the number of disturbances occurring per unit time. For purposes of comparison the same value of ℓ = 11.3 earth radii was chosen with one such impulse occurring every ten minutes. This represents the minimum diffusion time obtainable for a disturbance of this amplitude, applied to the

particle under consideration. The same diffusion time is obtained using any values of ℓ and $\frac{dn}{dt}$ which give the same value of $\ell^8 / \frac{dn}{dt}$. For example, forty-gamma disturbances occurring at approximately 90-minute intervals would give the same diffusion time as the ten-gamma disturbances occurring at ten-minute intervals.

We see that for both models diffusion will proceed much more rapidly at high L-values than at the more stable lower shells. There is one range of L-values for which the diffusion times for the sinusoidal model are approximately a factor of ten smaller than the diffusion times of the sudden disturbance model. This range of L-values is centered around the L-value at which the disturbance period is approximately equal to the drift period and resonance occurs. In particular, disturbances with periods of from ten to twenty minutes would appear to be most effective on the electrons we are considering between L = 3.4 and L = 4.8. To make an accurate estimate of the apparent rate of diffusion in this region, it would be necessary to consider the convective part of the particle motion also, which would require a knowledge of $\langle \Delta R \rangle$. However, the increase in diffusion time by over an order of magnitude between L = 4.8 and L = 3.4 is in qualitative agreement with the observed electron behavior. The amplitude of the disturbances required to produce the observed diffusion can be estimated using (4.23). The value of $\langle (\Delta R)^2 \rangle$ which is required for $\alpha = 0.4\ R_E$ and t = 1 day can be calculated and is found to be $0.08\ R_E^2$ /day. The amplitude necessary to produce this value of $\langle (\Delta R)^2 \rangle$ for a disturbance period of ten minutes is 4.5 gamma at a radial distance of $4\ R_E$ on the earth-sun line. In a

similar fashion it is found that an amplitude of 3 gamma at $4\ R_E$ is required for $a = 0.03\ R_E$, when t = 1 day at L = 3.4. Thus, it would appear that disturbances with periods of the order of ten minutes and amplitudes of a few gamma are capable of producing the observed diffusive behavior.

The diffusion times of the sinusoidal model increase as we move from larger toward smaller L-values and approach infinity at the L-value corresponding to the first minimum in the $\langle (\Delta R)^2 \rangle$ versus Ω/ω curve (Figure 16). Diffusion times for L-values corresponding to points beyond this first minimum are not shown in Figure 17.

D. Summary

The principal effect of the violation of the third invariant is to produce diffusion of particles radially across magnetic shells. A model applicable to disturbances with a rise time rapid compared to the drift period of the particles under consideration has been treated previously by Parker and by Davis and Chang. In the present work we have considered a model representing a large-scale sinusoidal disturbance. Calculation of the mean square change in the geocentric particle distance and the characteristic diffusion time which can be obtained from this quantity indicates the existence of a resonance behavior when the period of the disturbance is approximately equal to the particle drift period. This indicates that relatively small amplitude sinusoidal disturbances can produce appreciable particle diffusion over a small range of L-values where the resonance effect is greatest.

Calculations have been carried out for characteristic diffusion times for 1.6 Mev electrons in the vicinity of $L = 4$, where an apparent diffusive behavior of electrons has been observed. The results indicate that the diffusion times predicted by the sinusoidal model can be approximately ten times smaller over a small range of L-values than those predicted by the sudden disturbance model, using the same amplitude. An accurate calculation of apparent drift velocities must include the convective part of the particle motion, which requires a knowledge of the mean change in the geocentric particle distance as well as the mean square change. To calculate the mean change in radial distance to the first non-vanishing order in R/ℓ requires an additional iteration of each calculation in the preceding section, which leads to such a voluminous amount of algebra as to be no longer tractable. However, the diffusion times calculated from $\langle (\Delta R)^2 \rangle$ appear to be of the right order of magnitude to give diffusion rates comparable to those observed when a disturbance amplitude of 5 gamma at $L = 4$ is assumed.

CHAPTER V

EXPERIMENTAL TESTS

We shall consider measurements which could be performed to make an experimental study of the processes which have been discussed theoretically in the previous chapters. Since controlled experimental conditions do not exist in the magnetosphere, there will generally be a number of acceleration and loss mechanisms simultaneously operative. For this reason it is somewhat difficult to isolate the effects produced by one particular mechanism. However, it should be possible to determine whether a given set of observations is consistent with an assumed model for a particular mechanism.

In order to ascertain whether the mechanisms we are considering are operative, we need to choose observational conditions under which the individual mechanisms can be separated out. The diffusion process across L-values associated with the violation of the third invariant will tend to be the most noticeable where a strong radial dependence of the particle flux exists. However, a radial dependence of a temporary nature, such as that associated with a magnetic storm, must be chosen since any steep radial dependence of a permanent or quasi-permanent nature such as the "slot" must imply conservation of the third invariant in order to persist.

Measurements of radial distribution of the particle flux should be made over a sufficiently long period of time to allow a characteristic time scale to be established for any apparent diffusion which may be present. The post-storm measurements of $E > 1.6$ Mev electrons given by Frank et al. (1964) which were discussed in Chapter IV provide a reasonable example of the type of measurement needed. Simultaneous magnetic field measurements should be made from which

a hydromagnetic wave frequency spectrum can be determined. The calculations of Chapter IV can be used to ascertain whether the observed wave amplitudes and particle diffusion rates are consistent with the assumed model.

For the example of $E > 1.6$ Mev electrons in the region $3 \leq L \leq 5$, the wave power spectrum of ΔB is required over a range of periods between five minutes and twenty minutes. Any abrupt drop-off in the power spectrum could result in a complete cessation in the apparent particle diffusion at some minimum L-value, so correlations of this type should also be attempted. The reason of such a cessation of particle diffusion can be seen by referring to Figure 17. The diffusion time associated with a given wave period takes a rather abrupt increase as it approaches a minimum L-value. For example, if the power spectrum dropped off sharply near some minimum period, say $T_{wave} \sim 10$ minutes, then the diffusion could be expected to stop at $L \sim 2.8$. An effort should be made to ascertain whether waves near one particular period persist over a sufficient period of time for the sinusoidal mechanism to be effective.

When the second invariant is violated, it is likely that the third invariant also will be violated at the same time. Therefore, the chances for observing the effects of violation of the second invariant would seem to be best under conditions where the radial dependence of the flux is not too great. The violation of the second invariant by the mechanism we are considering produces a random walk of particle mirror points down the field line, but no motion across field lines can occur. Correlated changes in energy and pitch angle are produced, and a depletion of the total number of particles trapped in the region can be expected. Correlated measure-

ments of both the field and particles are required. Characteristic life times can be estimated using the calculations of Chapter III, if the hydromagnetic wave spectrum is known and these times can be compared with the observed time scale of depletion. It will be necessary to obtain some information on the particle energy spectrum in order to carry out this test. An instrument which detects only all particles above a given energy threshold might show an increased counting rate, even though the number of trapped particles is decreasing due to particles with energies just below the threshold being accelerated above the threshold before they are lost from the trapped region. This could be troublesome when the energy spectrum is steep.

The range of periods over which the hydromagnetic wave frequency spectrum is required depends on the energy range of the particles being investigated. For example, to study the effectiveness of the mechanism on electrons with energies of tens of kilovolts, an accurate wave frequency spectrum in the range of wave periods between one and 10 seconds would be required at $L \sim 4$. The same wave measurements would also be applicable to the study of protons with energies from one to several tens of Mev at the same L-value. In order to correlate wave activity with the behavior of protons with energies of the order of hundreds of kilovolts, the wave spectrum between 10 seconds and 60 seconds is required. In particular, the spectrum of ΔB, the difference between the field strength and its ambient value is the quantity desired. Since the characteristic lifetime is inversely proportional to the square of ΔB, it is necessary to be able to deduce this quantity to within a few gammas.

An additional check on the mechanism can be made by comparing the pitch angle distribution before and after a period of magnetic disturbances. The concentration at higher pitch angles should be reduced due to migration of particle mirror points down the field lines.

CHAPTER VI

SUMMARY AND DISCUSSION

A. Summary

In this study we have considered two possible mechanisms by which the geomagnetically trapped energetic particles can interact with hydromagnetic perturbations. These include violation of the longitudinal invariant by small-amplitude hydromagnetic waves and violation of the flux invariant by large scale magnetic disturbances. These mechanisms were chosen because it would appear that they must be operative, at least to some extent, whenever magnetic perturbations are present in the magnetosphere.

Preliminary to the main study, the three fundamental periods of the trapped particle motion were discussed, and values for these periods were calculated for a wide energy range for both electrons and protons for a number of L-values. These periods are presented in both tabular and graphical form and are used to make an estimate of the range of hydromagnetic wave periods required to violate the three invariants.

Violation of the second invariant by small-amplitude waves was investigated, using a model originally employed by Parker. In the original analysis a restriction that the ratio of the bounce period to the wave period be less than one was imposed. In the present work this restriction has been removed, making it possible to estimate characteristic lifetimes as a function of particle energy. Sample calculations of characteristic lifetimes and diffusion times were made for several examples which have practical applications to problems in the magnetosphere. These calculations indicate that

waves with periods in the 10-sec to 60-sec range can provide an important loss mechanism for protons in the energy range of 100 kev to several Mev for $L \sim 4$ and greater. For $L < 4$ the proton lifetimes limited by charge exchange and Coulomb scattering as calculated by Liemohn (1961) appear to be shorter than those limited by hydromagnetic waves unless very large wave amplitudes are assumed. Similar calculations for electrons indicate that magnetic disturbances with periods from 10 seconds down to one second or less can provide an effective loss mechanism for particles in an energy range from tens of kev to several Mev. The characteristic lifetimes for both electrons and protons decrease rapidly with increasing L-value, indicating lower stability in the outer parts of the magnetosphere.

The problem of the violation of the third invariant by small amplitude long-period disturbances was pursued by reviewing work previously done by Parker and by Davis and Chang. In this work, which was intended to treat particle perturbations produced by magnetic storms, a model was used in which a conducting plane was brought up abruptly from infinity to a magnetic dipole and held in place for a time long in comparison to the particle drift periods. This model would seem to be adequate for the treatment of storm-type disturbances and perhaps for sudden impulses. However, it is desirable to be able to treat sinusoidal waves for purposes of comparison with the power spectra of magnetic disturbances and to investigate the possibility of resonance effects. Accordingly, in the present work a model was used in which a dipole field is perturbed by an image dipole whose moment has a sinusoidal time dependence. In order to use such a model, it is necessary to calculate the EXB drift velocity produced by the induced electric field. This was

done by following the motion of the thermal plasma which moves with the lines of force. In this way it was possible to obtain the drift behavior of individual particles and to finally obtain the mean square change in the particle radial distance per disturbance $\langle (\Delta R)^2 \rangle$ by considering an ensemble of particles. The dependence of $\langle (\Delta R)^2 \rangle$ on wave period shows a pronounced resonance behavior when the wave period approaches the particle drift period.

Using the mean square change in geocentric particle distance, the characteristic times for diffusion of particles across L-values could be estimated. As an example, diffusion times for electrons which would have an energy of 1.6 Mev at L = 4 were calculated, assuming a disturbance amplitude of $\sim 5\ \gamma$ at a geocentric distance of four earth radii on the earth-sun line. Disturbance periods from five minutes to 20 minutes were considered. For purposes of comparison, diffusion times were calculated, using the sudden-disturbance model with a similar disturbance amplitude. It was assumed that one such disturbance occurred every ten minutes, which is an unrealistically large number but serves to define the smallest possible diffusion times which could be obtained with this model. It was found that for L-values near which the resonance condition was satisfied (disturbance period approximately equal to the particle drift period), diffusion times calculated from the sinusoidal model were as much as a factor of ten smaller than those calculated from the sudden model, indicating sinusoidal disturbances can be more efficient in producing diffusion for particles of a given energy over a limited range of L-values. The sinusoidal diffusion times were found to increase abruptly as a minimum L-value is approached, indicating that an abrupt decrease in particle diffusion would be expected at such a point.

Finally, measurements were proposed which could be used to study the two mechanisms experimentally. The lack of controlled experimental conditions in the magnetosphere makes it difficult to separate out individual mechanisms which may be operative at a given time. Since violation of the third invariant produces radial diffusion, the effect will be most pronounced where a steep radial dependence of the particle distribution exists. Therefore, strong temporary radial flux dependencies such as those observed for $E > 1.6$ Mev electrons under post-magnetic storm conditions seem to provide the best circumstances under which to observe violation of the third invariant. In order for the sinusoidal model to operate at maximum effectiveness, it is necessary that a significant number of waves be present with periods within a few minutes of the particle drift periods during the time of magnetically disturbed conditions. This should be checked by making determinations of the frequency spectra of $\triangle B$ throughout the time when disturbed conditions exist.

Violation of the second invariant should best be observed where the radial distribution of the particle flux is slight in order to minimize the effects of third invariant violation. Efforts should be made to observe particle depletion in such regions during magnetically disturbed conditions and to compare the observed characteristic decay times with the characteristic times calculated in Chapter III. It should also be possible to detect a change in pitch angle distribution during a disturbed period if the mechanism is operative, due to migration of particle mirror points down the lines of force. The energy ranges in which particle measurements would be required, along with the appropriate ranges of wave periods over which wave spectra are needed, are given in Chapter V.

B. Limitations of the Study and Suggestions for Further Investigation

The principal limitations of the study of the violation of the second invariant by hydromagnetic waves lie in the model used. As has been pointed out, the wave amplitude of the model increases down the field line, while a decreasing amplitude would probably be more realistic. This would tend to cause the characteristic times to be underestimated somewhat, especially for particles with large initial pitch angles, since the effectiveness of the mechanism would be overestimated toward the lower part of the field line. A second disadvantage of the model is that the field lines converge less rapidly than the field lines in a dipole field. This results in the dependence of the bounce period of the particle on the parallel component of velocity being somewhat different in the two cases.

Any attempt to correct either of the difficulties mentioned above appears to result in a model for which the individual particle motion is too complicated to be treated analytically, so it would become necessary to resort to lengthy numerical analysis. The model used in this work appears adequate to serve as a guide line in estimating the effectiveness of the mechanism and in planning an experimental study of the mechanism, and it can be used for making rough correlations of field and particle data. However, when more complete data become available, it may be of interest to attempt similar studies with more sophisticated models.

In the treatment of violation of the third invariant, only particles mirroring in the equatorial plane (90° pitch angle) were considered. The inclusion of particles with pitch angles less than

90° greatly complicates the problem and would not appear to lead to physical results appreciably different from those obtained with the simpler model. Comparison of the amplitudes of large-scale magnetic disturbances at satellite altitudes with the amplitudes at ground level indicates that the accurate representation of such disturbances may require models more complicated than an image dipole (Cahill and Nishida, 1964). However, the dipole model should suffice to treat particle diffusion over a limited range of L-values when the amplitude of the magnetic disturbance is specified in the region of diffusion. In order to provide a complete statistical description of the particle motion, using the Fokker-Planck formulation, the mean change in geocentric particle distance is required in addition to the mean square change. The treatment of sinusoidal disturbances provided in this work, along with the treatment of sudden disturbances given by Davis and Chang should be adequate to serve as guide lines for experimental studies and to provide a means for attempting a rough correlation between magnetic field and particle data. As in the case of the violation of the longitudinal invariant, more sophisticated treatments of the problem may be warranted as more complete data become available.

BIBLIOGRAPHY

1. Alfvén, H. "Hydromagnetics of the magnetosphere," Sp. Sci. Reviews 2, 862-870 (1963).

2. Axford, W. I., and C. O. Hines, "A unifying theory of high-latitude geophysical phenomena and geomagnetic storms," Can. J. Phys. 39, 1433-1464 (1964).

3. Beard, D. B., "The solar wind geomagnetic field boundary," Rev. Geophys. 2, 335-363 (1964).

4. Cahill, L. J. Jr., and P. G. Amazeen, "The boundary of the geomagnetic field," J. Geophys. Res. 68, 1835-1842 (1963).

5. Cahill, L. J., Jr., and A. Nishida, "Sudden impulses in the magnetosphere observed by Explorer 12," J. Geophys. Res. 69, 2243-2255 (1964).

6. Chandrasekhar, S., "Stochastic problems in physics and astronomy," Rev. Mod. Phys. 15, 31-42 (1943).

7. Coleman, P. J., "The effects of betatron accelerations upon the intensity and energy spectrum of magnetically trapped particles," J. Geophys. Res. 66, 1351-1361 (1961).

8. Cornwall, J. M., "Scattering of energetic trapped electrons by VLF waves," J. Geophys. Res. 69, 1251-1258 (1964).

9. Davis, L., and D. B. Chang, "On the effect of geomagnetic fluctuations on trapped particles," J. Geophys. Res. 67, 2169-2179 (1962).

10. Davis. L. R., and J. M. Williamson, "Low energy trapped protons," NASA/GSFC Report #X-611-62-89 (Presented at COSPAR Meeting, Washington, D. C., April 30 to May 9, 1962a).

11. Davis, L. R., and J. M. Williamson, "Low energy trapped protons," Space Research (edited by W. Priester) III, North-Holland Publishing Co., Amsterdam, pp. 365-375 (1962b).

12. Dessler, A. J., "Length of the magnetospheric tail," J. Geophys. Res. 69, 3913-3918 (1964).

13. Dessler, A. J., and R. Karplus, "Some effects of diamagnetic ring currents on Van Allen radiation," J. Geophys. Res. 66, 2289-2295 (1961).

14. Dragt, A. J., "Effect of hydromagnetic waves on the lifetime of Van Allen radiation protons," J. Geophys. Res. 66, 1641-1649 (1961).

15. Dungey, J. W., Cosmic Electrodynamics (Cambridge University Press, Oxford, 1958), Chaps. 6.4 and 8.4.

16. Dungey, J. W., "Loss of Van Allen electrons due to whistlers," Planetary & Space Sci. 11, 591-595 (1963).

17. Fermi, E., "On the origin of cosmic radiation," Phys. Rev. 75, 1169-1174 (1949).

18. Frank, L. A., J. A. Van Allen, and H. K. Hills, "A study of charged particles in the earth's outer radiation zone with Explorer 14," J. Geophys. Res. 69, 2171 (1964).

19. Frank, L. A., "Apparent, inward radial diffusion of electrons $E > 1.6$ Mev in the outer radiation zone (Explorer 14)," Trans. AGU 46, 137 (1965).

20. Gold, T., "Motions of the magnetosphere of the earth," J. Geophys. Res. 64, 1219-1224 (1959).

21. Hamlin, D. A., R. Karplus, R. C. Vik, and K. M. Watson, "Mirror and azimuthal drift frequencies for geomagnetically trapped particles," J. Geophys. Res. 66, 1-4 (1961).

22. Helliwell, R. A., and R. F. Bell, "A new mechanism for accelerating electrons in the outer ionosphere," J. Geophys. Res. 65, 1839-1842 (1960).

23. Herlofson, N., "Diffusion of particles in the earth's radiation belts," Phys. Rev. Letters 5, 414-416 (1960).

24. Hess, W. N., "High energy outer belt protons," Trans. AGU 46, 142 (1965).

25. Jahnke, E. and F. Emde, Tables of Functions (Dover Publications, New York, 1945) 4th edition.

26. Johnson, F. S., "The gross character of the geomagnetic field in the solar wind," J. Geophys. Res. 65, 3049 (1960).

27. Kaufmann, R. L., "Experimental tests for the acceleration of trapped particles," J. Geophys. Res. 68, 371-386 (1963).

28. Lenchek, A. M., and S. F. Singer, "Geomagnetically trapped protons from cosmic-ray albedo neutrons," J. Geophys. Res. 67, 1263-1285 (1962).

29. Liemohn, H., "The lifetime of radiation belt protons with energies between 1 kev and 1 Mev," J. Geophys. Res. 66, 3593-3595 (1961).

30. Mead, G. D., and D. B. Beard, "Shape of the geomagnetic field solar wind boundary," J. Geophys. Res. 69, 1169-1179 (1964).

31. Nakada, M. P., and G. D. Mead, "Diffusion of protons in the outer radiation belt," NASA/GSFC Pub. No. X-640-65-273 (1965).

32. Northrop, T. G., and E. Teller, "Stability of the adiabatic motion of charged particles in the earth's field," Phys. Rev. 117, 215 (1960).

33. Northrop, T. G., "Adisbatic charged-particle motion," Rev. of Geophys. 1, 283 (1963a).

34. Northrop, T. G., The Adiabatic Motion of Charged Particles (Interscience Publishers, New York, 1963b).

35. Obayashi, T., "The streaming of solar flare particles and plasma in interplanetary space," Sp. Sci. Rev. 3, 79-108 (1964).

36. Parker, E. N., "Interaction of the solar wind with the geomagnetic field," Phys. Fluids 1, 171-187 (1958).

37. Parker, E. N., "The hydrodynamic theory of solar corpuscular radiation and stellar winds," Astrophys. J. 132, 821 (1960a).

38. Parker, E. N., "Geomagnetic fluctuations and the form of the outer zone of the Van Allen radiation belt," J. Geophys. Res. 65, 3117-3130 (1960b).

39. Parker, E. N., "Effect of hydromagnetic waves in a dipole field on the longitudinal invariant," J. Geophys. Res. 66, 693-708 (1961a).

40. Parker, E. N., "Transresonant electron acceleration," J. Geophys. Res. 66, 2673-2676 (1961b).

41. Parker, E. N., "The scattering of charged particles by magnetic irregularities," J. Geophys. Res. 69, 1755-1758 (1964).

42, Patel, V. L., "Low frequency hydromagnetic waves in the magnetosphere," UNH Report 64-5 (1964), (to be published in Planetary & Space Sci.).

43. Stormer, K., The Polar Aurora (Oxford University Press, London, 1955).

44. Van Allen, J. A., G. H. Ludwig, E. C. Ray, and C. E. McIlwain, "Observation of high intensity radiation by satellites 1958 Alpha and Gamma," Jet Propulsion 28, 588-592 (1958).

45. Wentzel, D. G., "Hydromagnetic waves and the trapped radiation: Part 1. Breakdown of the adiabatic invariance," J. Geophys. Res. 66, 359-362 (1961a).

46. Wentzel, D. G., "Hydromagnetic waves and the trapped radiation: Part 2. Displacements of mirror points," J. Geophys. Res. 66, 363-369 (1961b).

47. Wentzel, D. G., "Hydromagnetic waves and the trapped radiation: Part 3. Effects on protons above the proton belt," J. Geophys. Res. 67, 485-498 (1962).

APPENDIX A

EVALUATION OF $\langle \Delta v_{\parallel} \rangle$ AND $\langle (\Delta v_{\parallel})^2 \rangle$

In order to calculate the velocity of the particle on its return to the origin, the time required for the particle to return must be obtained by finding the roots of (3.9) with s set equal to zero, i.e.,

$$v_{o_{\parallel}} t - \frac{v_{o_\perp}^2 t^2}{4a} + \frac{v_{o_\perp}^2 \mathcal{E}}{2a\omega}\left[\sin(\omega t - \mathcal{S}) - \omega t \cos\mathcal{S} + \sin\mathcal{S}\right] = 0 \qquad (A.1)$$

If the unperturbed case is considered ($\mathcal{E} = 0$), it is obvious from (A.1) that the time required for the particle to return to S = 0 is $4a v_{o_{\parallel}} / v_{o_\perp}^2$ which we shall call T_m. In terms of T_m, (A.1) can be rewritten

$$(\omega t)^2 - (\omega T_m)(\omega t) - 2\mathcal{E}\left[\sin\omega t \cos\mathcal{S} - \cos\omega t \sin\mathcal{S} - \omega t \cos\mathcal{S} + \sin\mathcal{S}\right] = 0 \qquad (A.2)$$

Assuming ωt can be expanded in the form of

$$\omega t = a_0 + a_1 \mathcal{E} + a_2 \mathcal{E}^2 + \ldots \qquad (A.3)$$

(A.2) can be written

$$\begin{aligned} &a_0(a_0 - \omega T_m) + \left[a_1(2a_0 - \omega T_m) - 2(\cos\mathcal{S}\sin a_0 \right. \\ &\left. - \sin\mathcal{S}\cos a_0 - a_0\cos\mathcal{S} + \sin\mathcal{S}\right]\mathcal{E} + \left[(2a_0a_2 \right. \\ &\left. + a_1^2 - a_2\omega T_m) - 2(a_1\cos\mathcal{S}\cos a_0 + a_1\sin\mathcal{S}\sin a_0 \right. \\ &\left. - a_1\cos\mathcal{S})\right]\mathcal{E}^2 + \ldots = 0 \end{aligned} \qquad (A.4)$$

where terms through order ϵ^2 have been retained. Since this relation must hold for arbitrary ϵ, the coefficient of each power of ϵ must vanish, giving the set of equations

$$
\begin{aligned}
&a_0(a_0 - \omega T_m) = 0 \\
&a_1(2a_0 - \omega T_m) = 2(\cos\delta \sin a_0 - \sin\delta \cos a_0 \\
&\qquad - a_0 \cos\delta + \sin\delta) \\
&a_2(2a_0 - \omega T_m) + a_1^2 = 2(a_1 \cos\delta \cos a_0 + a_1 \sin\delta \sin a_0 \\
&\qquad - a_1 \cos\delta)
\end{aligned}
\tag{A.5}
$$

Discarding the trivial solution $a_0 = 0$, the set of equations (A.5) can be solved for a_0, a_1, and a_2, giving

$$
\begin{aligned}
&a_0 = \omega T_m \\
&a_1 = \frac{2}{\omega T_m} (\cos\delta \sin \omega T_m - \sin\delta \cos \omega T_m \\
&\qquad - \omega T_m \cos\delta + \sin\delta) \\
&a_2 = \frac{1}{\omega T_m} (2a_1 \cos \omega T_m \cos\delta + 2a_1 \sin \omega T_m \sin\delta \\
&\qquad - 2a_1 \cos\delta - a_1^2)
\end{aligned}
\tag{A.6}
$$

This determines the time required for the particle to return to the origin through order ϵ^2. The calculation could be carried to higher order in ϵ if desired, but this is not necessary for our purpose.

The time calculated above is now substituted into (3.8) to obtain the change in the parallel component of velocity compared to its initial value. After simplification and rearrangement, this becomes

$$
\Delta v_{0_{\parallel}} = \frac{2}{\omega T_m} \epsilon \left[a_1 - \cos \omega T_m \cos\delta - \sin \omega T_m \sin\delta \right. \tag{A.7}
$$

$$+ \cos \delta \Big] + \frac{2}{\omega T_m} \varepsilon^2 \Big[\frac{a_2}{2} + a_1 \sin \omega T_m \cos \delta$$

$$a_1 \cos \omega T_m \sin \delta \Big] + \theta(\varepsilon^3) \tag{A.7}$$

The square of the change in velocity is simply

$$(\Delta v_{11})^2 = \frac{4}{\omega T_m)^2} \varepsilon^2 \Big[a_1 - \cos \omega T_m \cos \delta$$

$$- \sin \omega T_m \sin \delta + \cos \delta \Big]^2 + \theta(\varepsilon^3) \tag{A.8}$$

Substitution of (A.7) into the definition of the mean velocity change (3.12) gives

$$\langle \Delta v_{11} \rangle = \frac{1}{2\pi T_m} \frac{2\varepsilon^2}{\omega T_m} \Big[\int_0^{2\pi} a_2 \, d\delta$$

$$+ \sin \omega T_m \int_0^{2\pi} a_1 \cos \delta \, d\delta - \cos \omega T_m \int_0^{2\pi} a_1 \sin \delta \, d\delta \Big] \tag{A.9}$$

since only terms in $\sin^2 \delta$ and $\cos^2 \delta$ contribute. Evaluation of the integrals and rearrangement of the terms result in equation (3.14). In a similar fashion substitution of (A.8) into the definition of the mean square velocity results in equation (3.15).

APPENDIX B

THE FOKKER-PLANCK EQUATION

The Fokker-Planck equation has been discussed extensively by Chandrasekhar (1943), and we shall follow his presentation here. For convenience let us consider a distribution of particles in a velocity space having only one dimension. Let $\Psi(u,t)\,du$ be the number of particles with velocities between u and u + du at time t. Then if $P(u;\Delta u)$ is the classical probability that a particle of velocity u will suffer an increase in velocity Δu time Δt we would expect $\Psi(u,\ t+\Delta t)$ to be given by

$$\Psi(u,\ t+\Delta t) = \int_{-\infty}^{\infty} P(u-\Delta u;\ \Delta u)\ \Psi(u-\Delta u,t)\quad d(\Delta u) - \int_{-\infty}^{\infty} P(u;\Delta u)\ \Psi(u,t)\quad d(\Delta u) \tag{B.1}$$

assuming there is no correlation between successive changes in velocity.

Now, if small changes in the velocity are most probable, then we can expand the functions in (B.1) in Taylor series, giving

$$\begin{aligned} \Psi(u,\ t+\Delta t) &= \Psi(u,t) + \frac{\partial \Psi}{\partial t}\Delta t \cdots \\ P(u-\Delta u;\Delta u) &= P(u;\Delta u) - \frac{\partial P}{\partial u}\Delta u + \frac{1}{2}\frac{\partial^2 P}{\partial u^2}(\Delta u)^2 + \cdots \\ \Psi(u-\Delta u,t) &= \Psi(u,t) - \frac{\partial \Psi}{\partial u}\Delta u + \frac{1}{2}\frac{\partial^2 \Psi}{\partial u^2}(\Delta u)^2 + \cdots \end{aligned} \tag{B.2}$$

Substitution of (B.2) into (B.1) gives, after some algebra,

$$\Psi(u,t) + \frac{\partial \Psi}{\partial t}\ \Delta t = \Psi(u,t)\int_{-\infty}^{\infty} P(u;\Delta u)\quad d(\Delta u) - \frac{\partial}{\partial u}\left[\Psi\int_{-\infty}^{\infty} P(u;\Delta u)\ \Delta u\, d(\Delta u)\right] + \frac{1}{2}\frac{\partial 2}{\partial u^2}\left[\Psi\int_{-\infty}^{\infty} P(u;\Delta u)\ \ (\Delta u)^2\ \ d(\Delta u)\right] \tag{B.3}$$

Assuming the classical transition probability is normalized to unity and making the following definitions,

$$\int_{-\infty}^{\infty} P(u;\Delta u)\ \Delta u\, d(\Delta u) \equiv \langle \Delta u \rangle \cdot \Delta t$$

$$\int_{-\infty}^{\infty} P(u;\Delta u)\ (\Delta u)^2\ d(\Delta u) \equiv \langle (\Delta u)^2 \rangle \cdot \Delta t \qquad \text{(B.4)}$$

we obtain

$$\frac{\partial \psi}{\partial t} = \frac{1}{2}\ \frac{\partial^2}{\partial u^2}\ \left[\psi \langle (\Delta u)^2 \rangle\right] - \frac{\partial}{\partial u}\left[\psi \langle \Delta u \rangle\right] \qquad \text{(B.5)}$$

which is the Fokker-Planck equation for our one-dimensional velocity space.

We see that (B.5) has the form of a diffusion equation with a term involving the first derivative of ψ added on. To obtain some idea of the physical significance of (B.5), consider the case when $\langle (\Delta u)^2 \rangle$ and $\langle \Delta u \rangle$ are constants. A particular solution of (B.5) is then

$$\psi(u,t) = N\pi^{-\frac{1}{2}} \left[2 \langle (\Delta u)^2 \rangle\ t\right]^{-\frac{1}{2}} \exp \left\{ \frac{\left[u-(u_0+\langle \Delta u \rangle t)\right]^2}{2 \langle (\Delta u)^2 \rangle\ t} \right\} \text{(B}$$

as may be verified by substitution into (B.5). This is the distribution function at time t for a system of N particles initially having a delta function distribution located at $u = u_0$.

The solution (B.6) is Gaussian in form, with an instantaneous "half-width" of $\left[2 \langle (\Delta u)^2 \rangle\ t\right]^{\frac{1}{2}}$ and instantaneous center of gravity located at $u_0 + \langle \Delta u \rangle\ t$. Thus, as time increases, the distribution spreads out as its center of gravity moves toward increasing u (assuming $\langle \Delta u \rangle$ is a positive quantity). When $\langle \Delta u \rangle$ is zero (B.5) reduces to the ordinary diffusion equation and (B.6) becomes a Gaussian with a fixed center of gravity undergoing a spread with

increasing time, with $\langle (\Delta u)^2 \rangle$ being a measure of the rate at which the spread occurs. Evidently then, the effect of the term involving $\langle \Delta u \rangle$ in (B.5) is to produce a convective motion of the particle distribution in velocity space, with $\langle \Delta u \rangle$ being a measure of the rate of this motion.

The form of the Fokker-Planck equation used in Chapter III is essentially the same as (B.5) with u replaced by $u_{o_{||}}$. In Chapter IV we are interested in the particle distribution in a one-dimensional space with the particle radial distance as the coordinate. However, the derivation of the appropriate Fokker-Planck equation is the same, essentially, as that outlined above.

APPENDIX C

CALCULATION OF THE FUNCTIONS F(x) AND G(x)

The calculations which lead to the functions F(x) and G(x) appearing in (3.24) and (3.32), respectively, are lengthy but straight forward. Details of these calculations are presented here.

To obtain the average value of $\langle \Delta \nu_{11} \rangle$ over a specified range of $x \equiv \omega T_m$, the integral which must be evaluated is

$$\int_{x_o}^{x_c} \langle \Delta \nu_{11} \rangle dx = \frac{2\nu\sigma_{11}\,\mathcal{E}^2}{T_m} - \left\{ \int_{x_o}^{x_c} \frac{\sin x}{x}\, dx \right.$$

$$+ \int_{x_o}^{x_c} \frac{(1-3\cos x)}{x^2}\, dx + 4\int_{x_o}^{x_c} \frac{\sin x}{x^3} dx \qquad (C.1)$$

$$\left. - 4\int_{x_o}^{x_c} \frac{(1-\cos x)}{x^4}\, dx \right.$$

The second integral on the right-hand side can be integrated by parts, giving

$$I_2 = \frac{(1-3\cos x_o)}{x_o} - \frac{(1-3\cos x_c)}{x_c} + 3\int_{x_o}^{x_c} \frac{\sin x}{x}\, dx \qquad (C.2)$$

The third integral on the right-hand side of (C.1) can be integrated by parts twice in succession to give

$$I_3 = \frac{\sin x_o}{2x_o^2} - \frac{\sin x_c}{2x_c^2} + \frac{\cos x_o}{2x_o} - \frac{\cos x_c}{2x_c} - \frac{1}{2}\int_{x_o}^{x_c} \frac{\sin x}{x}\, dx \qquad (C.3)$$

The fourth integral on the right-hand side of (C.1) can be integrated by parts, yielding

$$I_4 = \frac{(1-\cos x_o)}{3x_o^3} - \frac{(1-3\cos x_c)}{3x_c^3} + \frac{1}{3}\int_{x_o}^{x_c} \frac{\sin x}{x^3}\, dx \qquad (C.4)$$

However, the remaining integral in (C.4) is just I_3 which has already been evaluated above. The only integrals now remaining are of the form

$$\int_{x_o}^{x_c} \frac{\sin x}{x} dx = Si(x_c) - Si(x_o) \qquad (C.5)$$

where Si(x) is the Sine Integral tabulated by Jahnke and Emde (1945).

Substituting (C.5), (C.4), (C.3), and (C.2) into (C.1), we obtain

$$\int_{x_o}^{x_c} \langle \Delta v_{11} \rangle dx = \frac{2 v_{o11} \mathcal{E}^2}{T_m} \left[F(x_c) - F(x_o) \right] \qquad (C.6)$$

where

$$F(x) = \frac{1}{3} \left[2Si(x) - \frac{(3-5 \cos x)}{x} - \frac{4 \sin x}{x^2} + \frac{4(1-\cos x)}{x^3} \right] \qquad (C.7)$$

By expressing the individual terms in their power series expansions, we find

$$F(x) \xrightarrow[x \to 0]{} \frac{5}{216} x^3 \qquad (C.8)$$

while the asymptotic form of the function is

$$F(x) \xrightarrow[x \to \infty]{} \frac{\pi}{3} - \frac{(1-\cos x)}{x} \qquad (C.9)$$

The integral which must be evaluated in calculating the average of $\langle (\Delta v_{11})^2 \rangle$ over a specified range of x is

$$\int_{x_o}^{x_c} \langle (\Delta v_{11})^2 \rangle dx = \frac{4 \mathcal{E}^2 v_{o11}^2}{\omega T_m^2} \left\{ \int_{x_o}^{x_c} \frac{(1 + \cos x)}{x} dx - 4 \int_{x_o}^{x_c} \frac{\sin x}{x^2} dx + 4 \int_{x_o}^{x_c} \frac{(1-\cos x)}{x^3} dx \right\} \qquad (C.10)$$

The first integral on the right-hand side can be reduced to the form

$$I_1' = \ln x_c - \ln x_o + \int_{x_o}^{x_c} \frac{\cos x}{x}\, dx \qquad (C.11)$$

The second integral on the right-hand side of (C.10) can be integrated by parts to give

$$I_2' = \frac{\sin x_o}{x_o} - \frac{\sin x_c}{x_c} + \int_{x_o}^{x_c} \frac{\cos x}{x}\, dx \qquad (C.12)$$

The third integral on the right-hand side of (C.10) can also be integrated by parts to give

$$I_3' = \frac{1}{2x_o^2} - \frac{1}{2x_c^2} + \frac{\cos x_c}{2x_c^2} - \frac{\cos x_o}{2x_o^2} + \frac{1}{2}\int_{x_o}^{x_c} \frac{\sin x}{x^2}\, dx \qquad (C.13)$$

The remaining integral in (C.13) is just I_2' which has already been evaluated. Thus, we have reduced the integrals to expressions containing integrals of the form

$$\int_{x_o}^{x_c} \frac{\cos x}{x}\, dx = Ci(x_c) - Ci(x_o) \qquad (C.14)$$

where Ci(x) is the Cosine Integral tabulated by Jahnke and Emde (1945) and defined as

$$Ci(x) \equiv \int_{\infty}^{x} \frac{\cos z}{z}\, dz \qquad (C.15)$$

Combining (C.14), (C.13), (C.12), and (C.11), we can write

$$\int_{x_o}^{x_c} \langle (\Delta v_{\parallel})^2 \rangle\, dx = \frac{4\mathcal{E}^2 v_{o\parallel}^2}{\omega T_m}\left[G(x_c) - G(x_o)\right] \qquad (C.16)$$

where G(x) is defined as

$$G(x) \equiv \ln(\gamma x) - 1 - Ci(x) + \frac{2\sin x}{x} - \frac{2(1-\cos x)}{x} \qquad (C.17)$$

The quantity $\ln \gamma = 0.577....$ is Euler's constant. Using the power series expansion and asymptotic form for Ci(x) given by Jahnke and Emde, we obtain

$$G(x) \xrightarrow[x \to o]{} \frac{x^4}{288} \qquad (C.18)$$

with the asymptotic form of G(x) being given by

$$G(x) \xrightarrow[x \to \infty]{} \ln x - \frac{0.423}{88} \qquad (C.19)$$

FIGURE CAPTIONS

Figure 1. The guiding center geometry. A charged particle located at position $\underline{r}$ with instantaneous velocity $\underline{v}$ and Larmor radius ρ has its guiding center located at $\underline{R}$.

Figure 2. Proton bounce periods. Curves of constant bounce period are shown on a plot of proton energy versus L-value. Rough estimates can be made of the time scale of the perturbations necessary to violate the second invariant of protons of a given energy at a particular L-value.

Figure 3. Electron bounce periods. Curves of constant bounce period are shown on a plot of electron energy versus L-value. Rough estimates can be made of the time scale of the perturbation necessary to violate the second invariant of electrons of a given energy at a particular L-value.

Figure 4. Proton drift periods. Curves of constant drift period are shown on a plot of proton energy versus L-value. Rough estimates can be made of the time scale of the perturbation necessary to violate the third invariant of protons of a given energy at a particular L-value.

Figure 5. First order Fermi acceleration. The magnetic field strength B as a function of distance along a field line s is shown schematically. Particles initially mirroring at a field strength B_{mirror} will be reflected from the wave as it moves down the field line and will undergo first order Fermi acceleration as a result.

Figure 6. Latitude of mirror point versus equatorial pitch angle. The calculations shown are for an earth-centered dipole field.

Figure 7. Mean change in the parallel velocity component versus ωT_m. The broken line indicates the approximation originally given by Parker.

Figure 8. Mean square change in the parallel velocity component versus ωT_m. The broken line indicates the approximation originally given by Parker.

Figure 9. The minimum equatorial pitch angle which a particle can assume (loss cone) versus equatorial distance to field line. The calculations shown are for an earth-centered dipole field with particle loss at the surface of the earth.

Figure 10. Proton characteristic lifetimes. The calculations shown are for an L-value of four, an initial equatorial pitch angle of 30°, and a wave amplitude of 10 γ at the mirror point. The curves are labeled according to the wave period assumed.

Figure 11. Electron characteristic lifetimes. The parameters used are the same as those used for protons in Figure 10, with the exception of the range of wave periods assumed.

Figure 12. Comparison of the characteristic lifetimes and characteristic diffusion times for protons. The calculations are for an L-value of four, initial pitch angle of 30°, and a wave amplitude at the mirror point of 10 γ.

Figure 13. Comparison of proton characteristic lifetimes for two different L-values. A wave period of 50 sec, wave amplitude of 10 γ at the mirror point, and an initial equatorial pitch angle of 30° were assumed.

Figure 14. The sudden disturbance model. A dipole field is perturbed by bringing a conducting plane up from infinity to a distance ℓ. The resulting perturbation field can be obtained by using an image dipole at a distance 2ℓ. The coordinate system used in the calculations is indicated.

Figure 15. Displacement of magnetic field lines in the sinusoidal model. The broken lines show the excursions of the field lines (greatly exaggerated) which intersect the equatorial plane along the solid circle when the perturbation is absent.

Figure 16. Mean square radial position of particles versus wave period. Resonance behavior is apparent in the region where the wave period and the drift period are comparable.

Figure 17. Electron diffusion times for a magnetic moment corresponding to an energy of 1.6 Mev at L = 4. The curves are labeled according to the wave period assumed in each case. The curve for the sudden disturbance model is shown for comparison.

GUIDING CENTER GEOMETRY

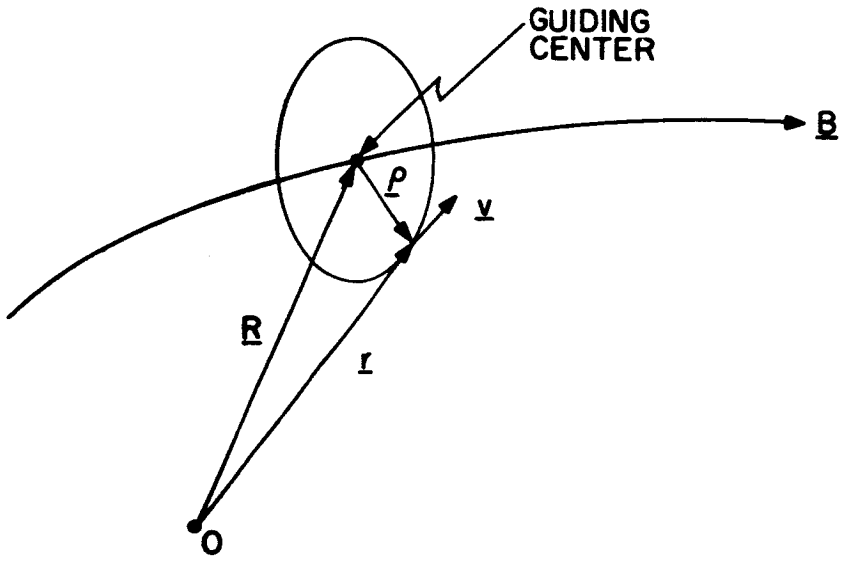

Figure 1

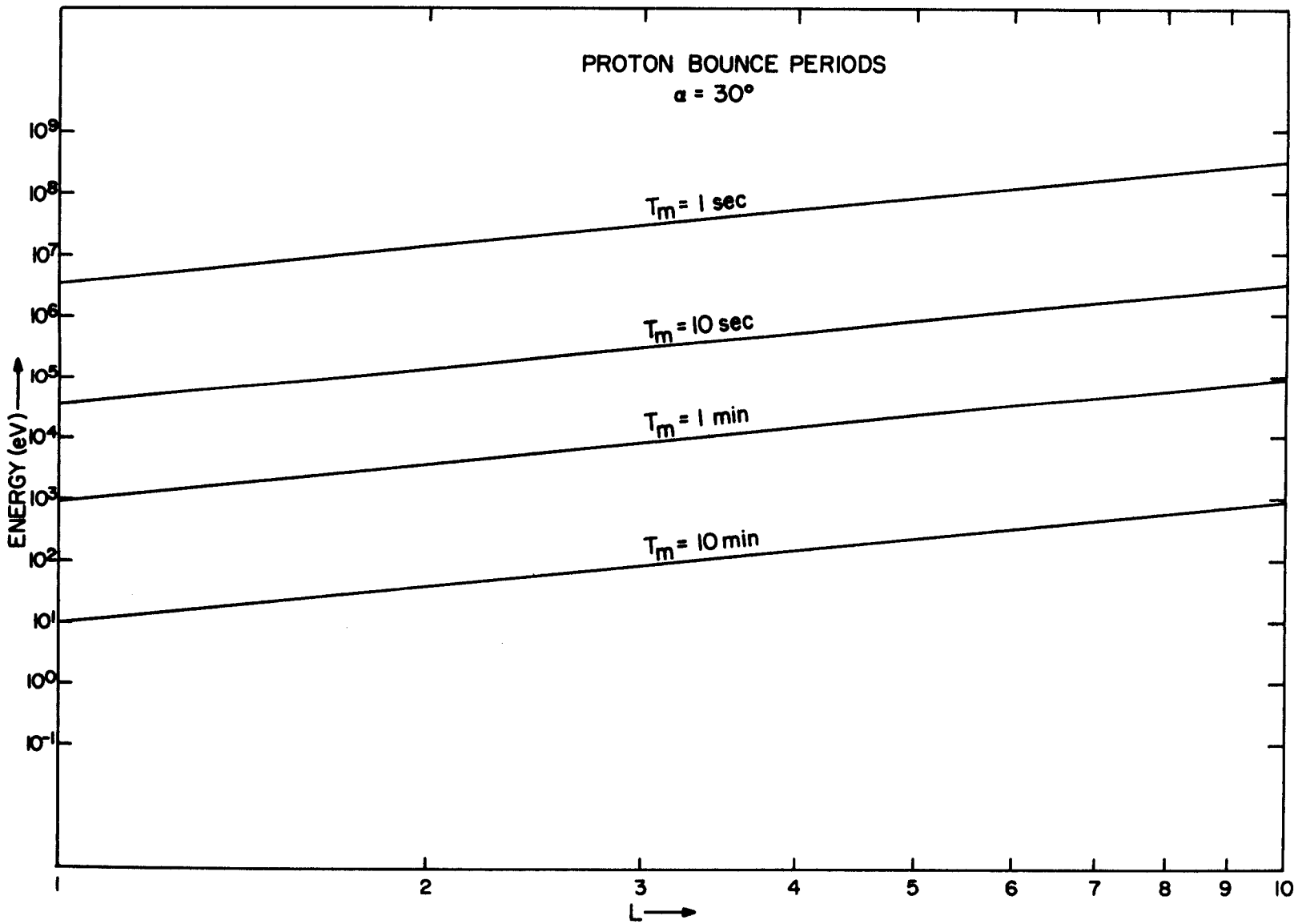
PROTON BOUNCE PERIODS
α = 30°
T_m = 1 sec
T_m = 10 sec
T_m = 1 min
T_m = 10 min
ENERGY (eV)
10^9
10^8
10^7
10^6
10^5
10^4
10^3
10^2
10^1
10^0
10^{-1}
1
2
3
4
5
6
7
8
9
10
L

Figure 2

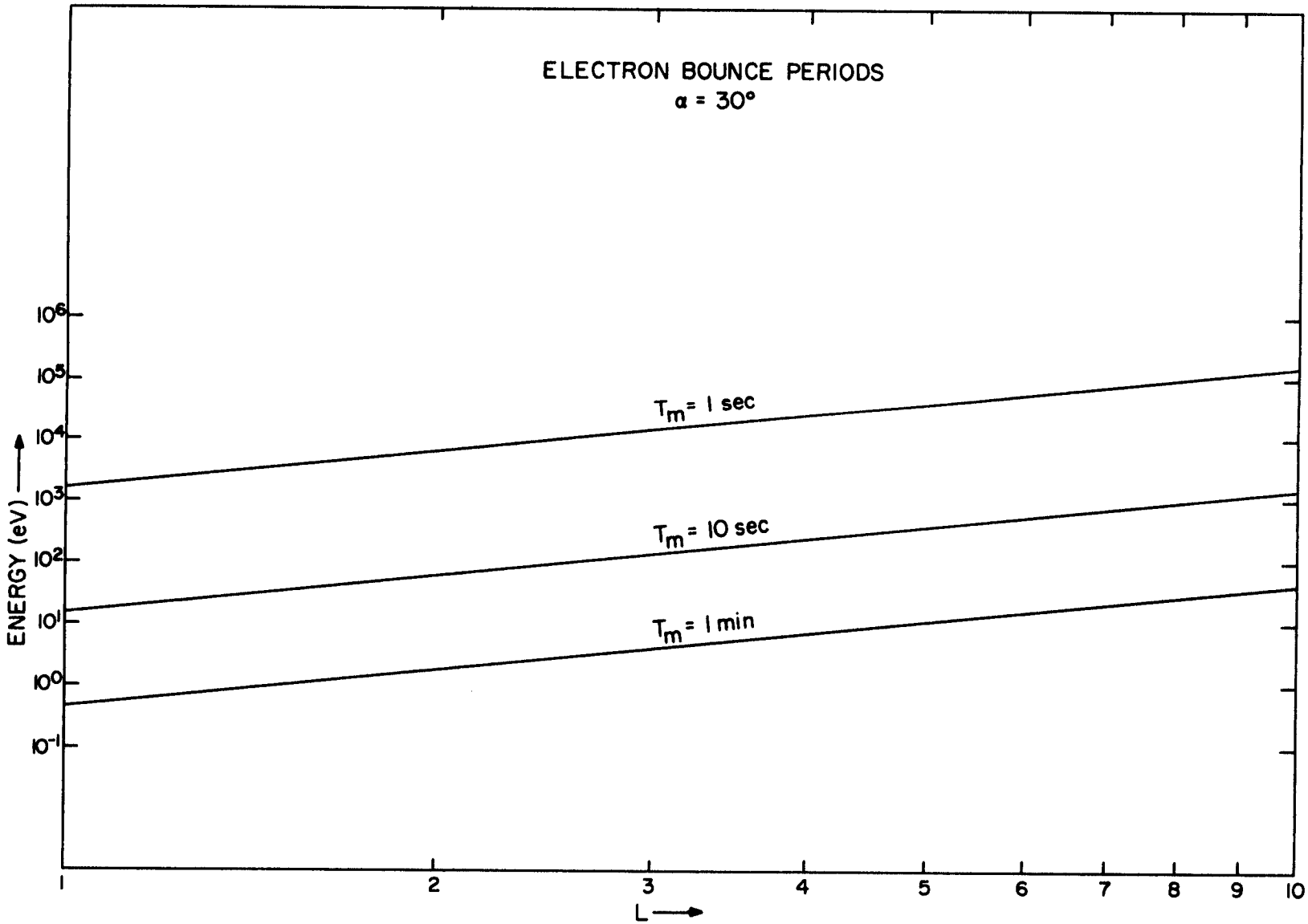
ELECTRON BOUNCE PERIODS
α = 30°
ENERGY (eV)
10^6
10^5
10^4
10^3
10^2
10^1
10^0
10^-1
T_m = 1 sec
T_m = 10 sec
T_m = 1 min
1
2
3
4
5
6
7
8
9
10
L

Figure 3

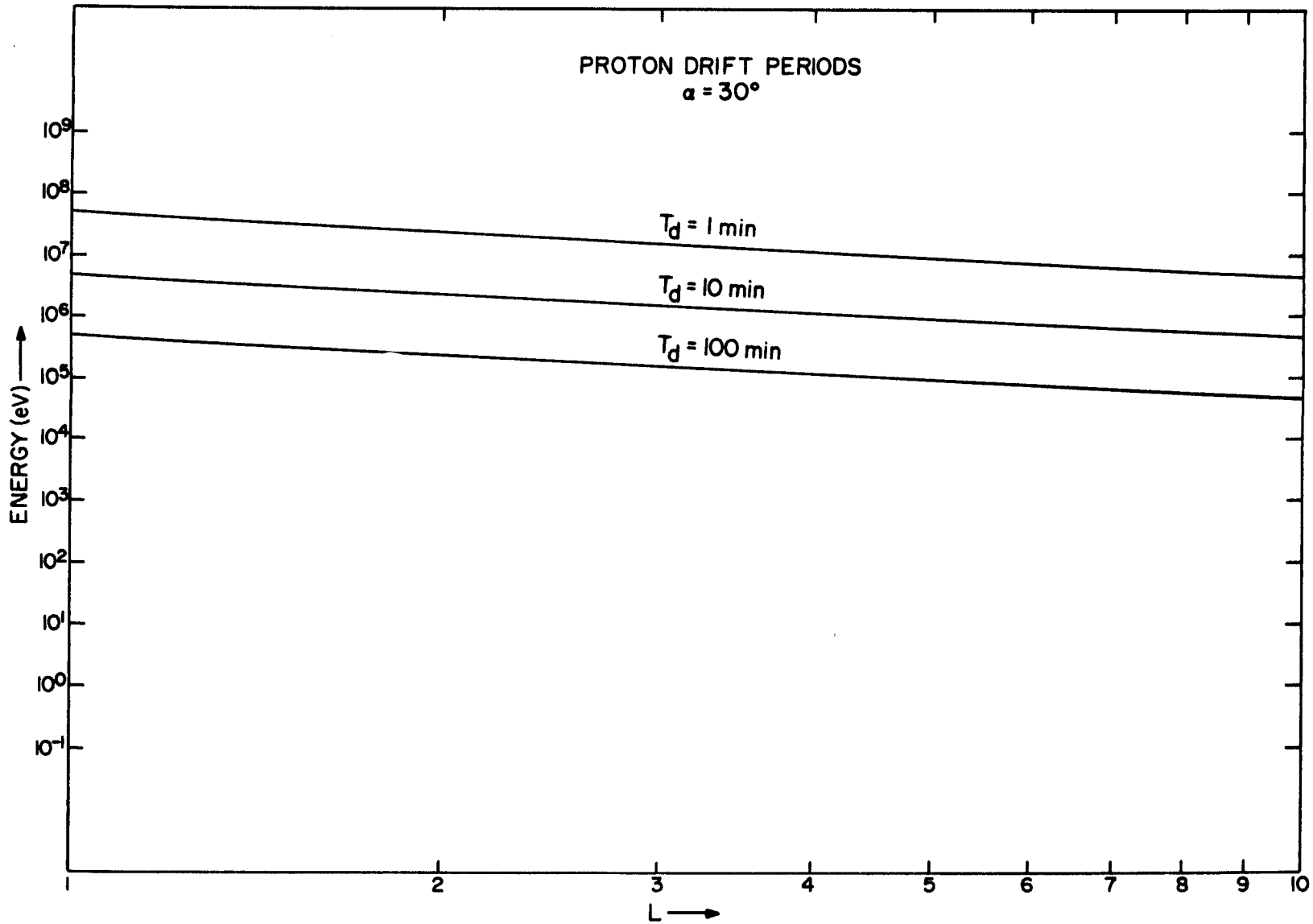
PROTON DRIFT PERIODS
α = 30°
T_d = 1 min
T_d = 10 min
T_d = 100 min
ENERGY (eV)
10^9
10^8
10^7
10^6
10^5
10^4
10^3
10^2
10^1
10^0
10^{-1}
1
2
3
4
5
6
7
8
9
10
L

Figure 4

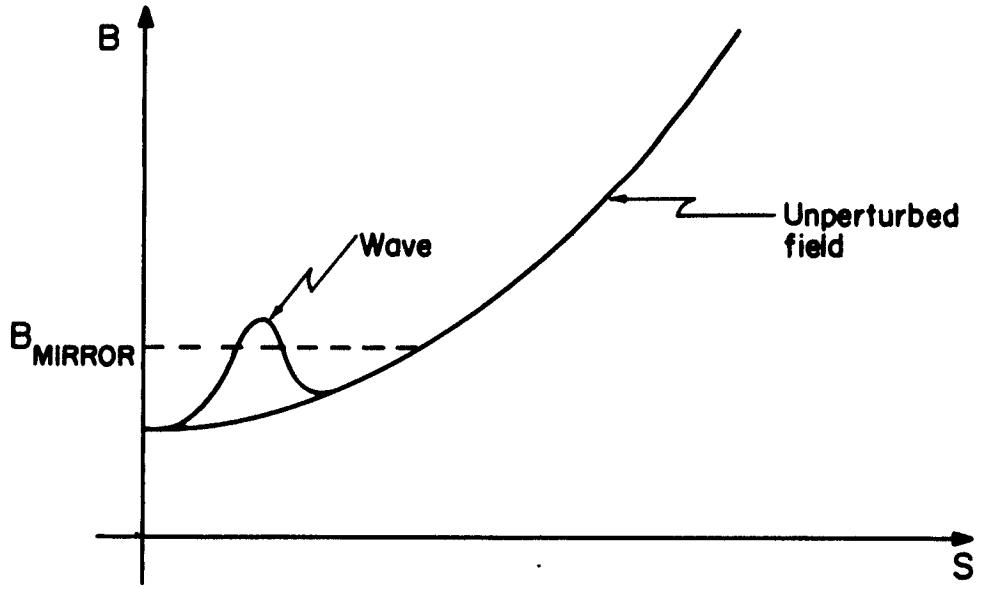

FIRST ORDER FERMI ACCELERATION

Figure 5

LATITUDE OF MIRROR POINT
VS
EQUATORIAL PITCH ANGLE

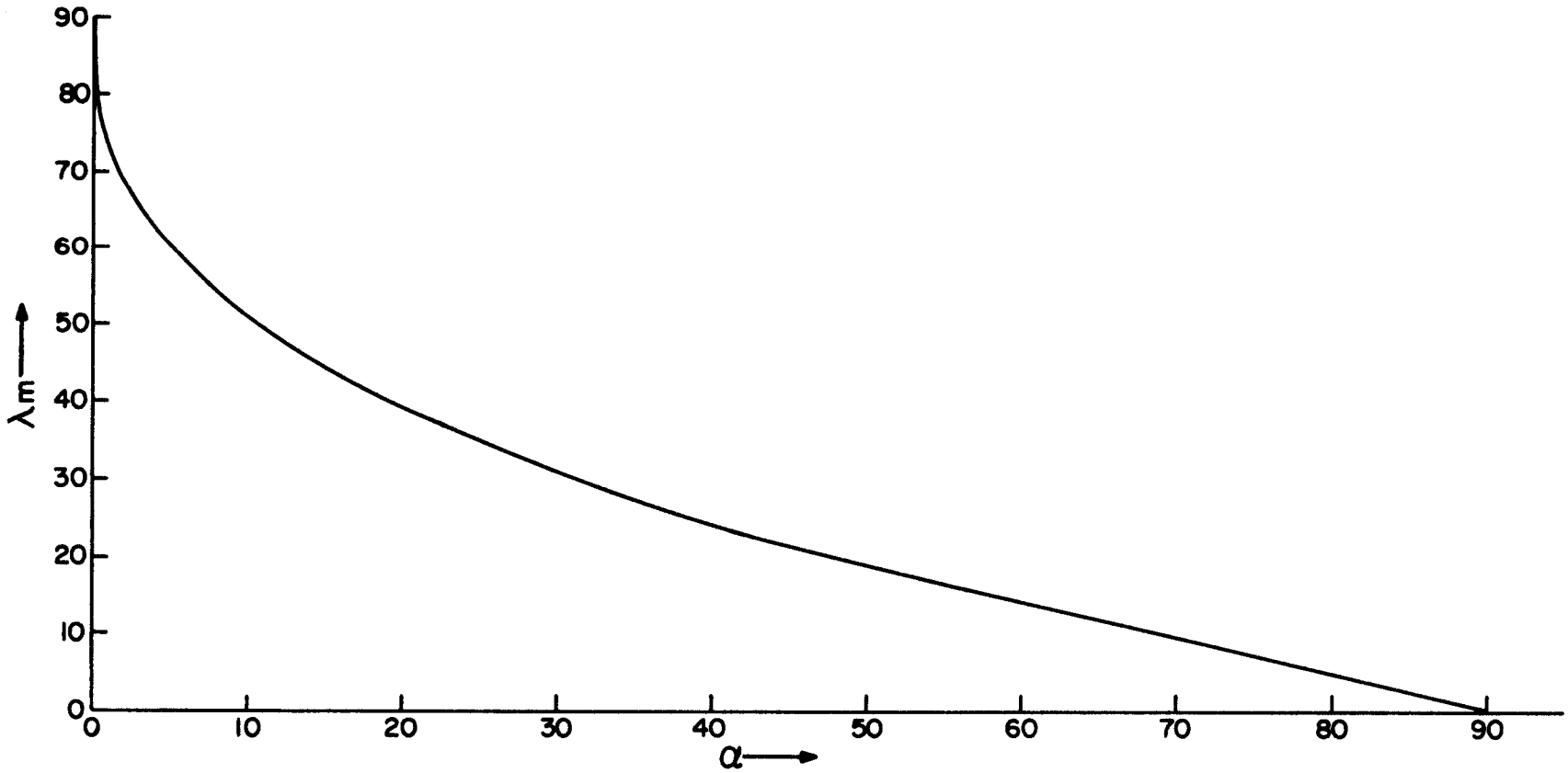

Figure 6

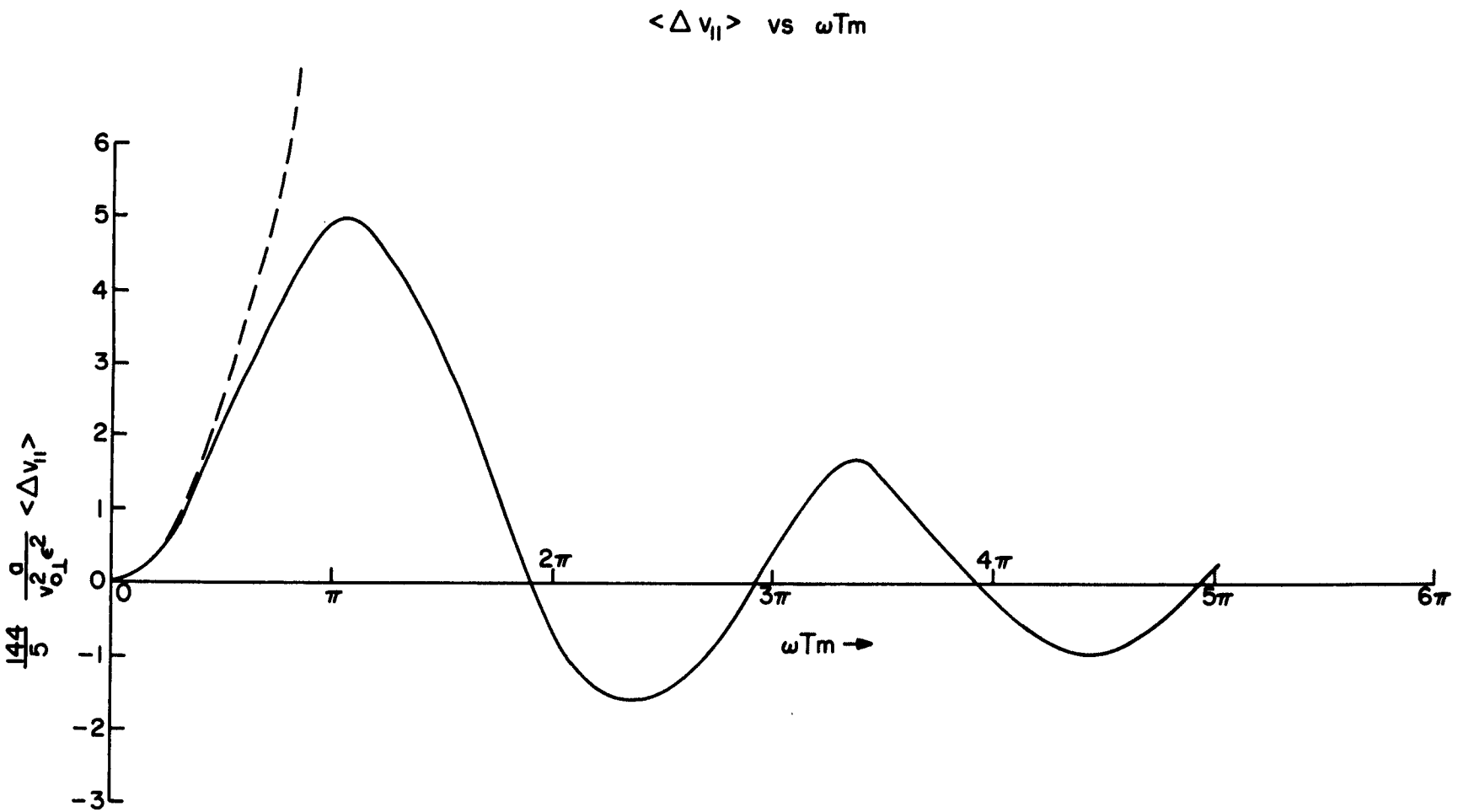
$\langle \Delta v_{\parallel} \rangle$ vs ωTm
$\frac{144}{5} \frac{a}{v_{o\perp}^2 e^2} \langle \Delta v_{\parallel} \rangle$
6
5
4
3
2
1
0
-1
-2
-3
0
π
2π
3π
4π
5π
6π
$\omega Tm \rightarrow$

Figure 7

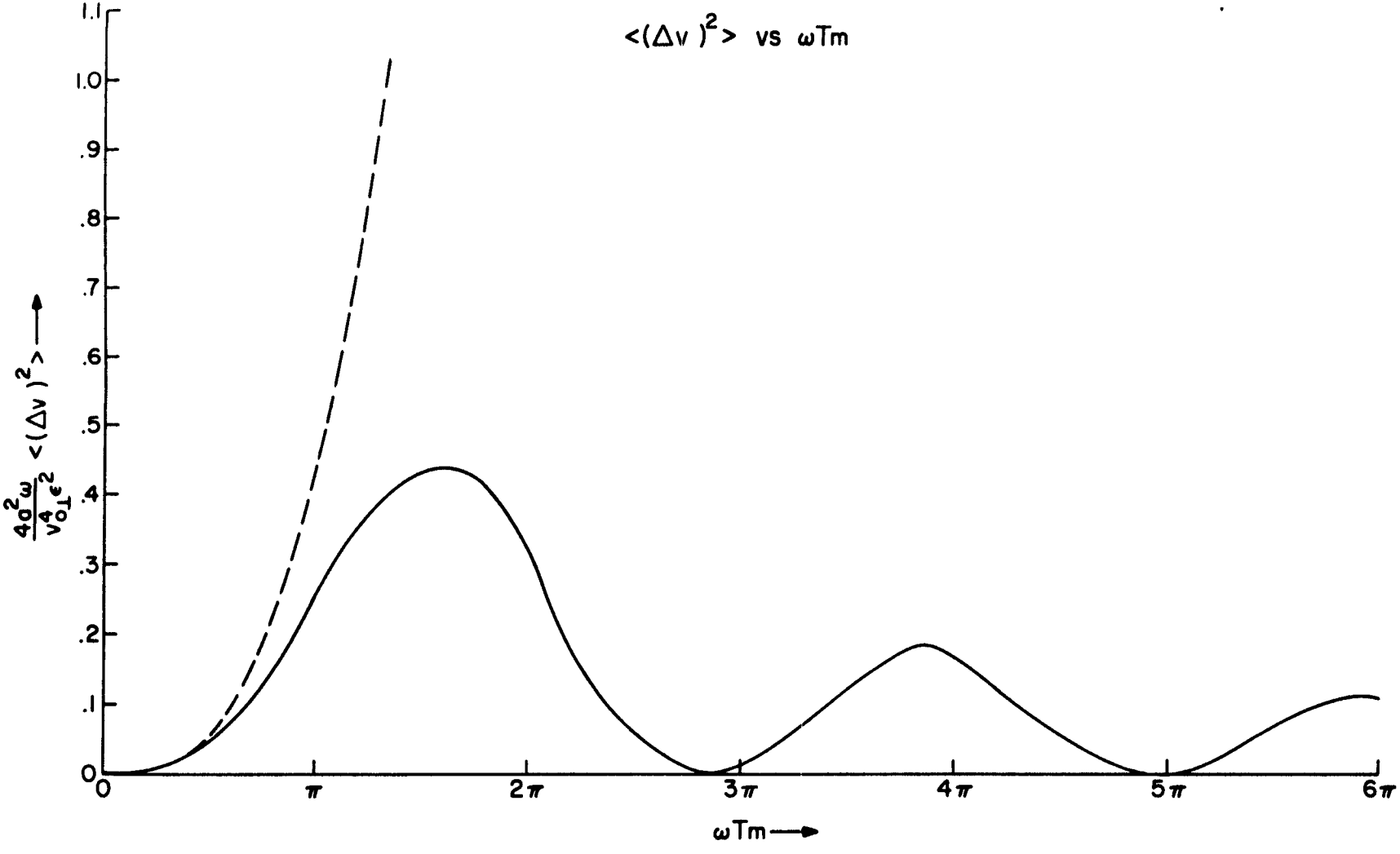
<(Δv)²> vs ωTm
1.1
1.0
.9
.8
.7
.6
.5
.4
.3
.2
.1
0
0
π
2π
3π
4π
5π
6π
ωTm
$\frac{4\sigma^2\omega}{v_{o\perp}^4\epsilon^2}\langle(\Delta v)^2\rangle$

Figure 8

MINIMUM EQUATORIAL PITCH ANGLE (LOSS CONE)
VS
EQUATORIAL DISTANCE TO FIELD LINE

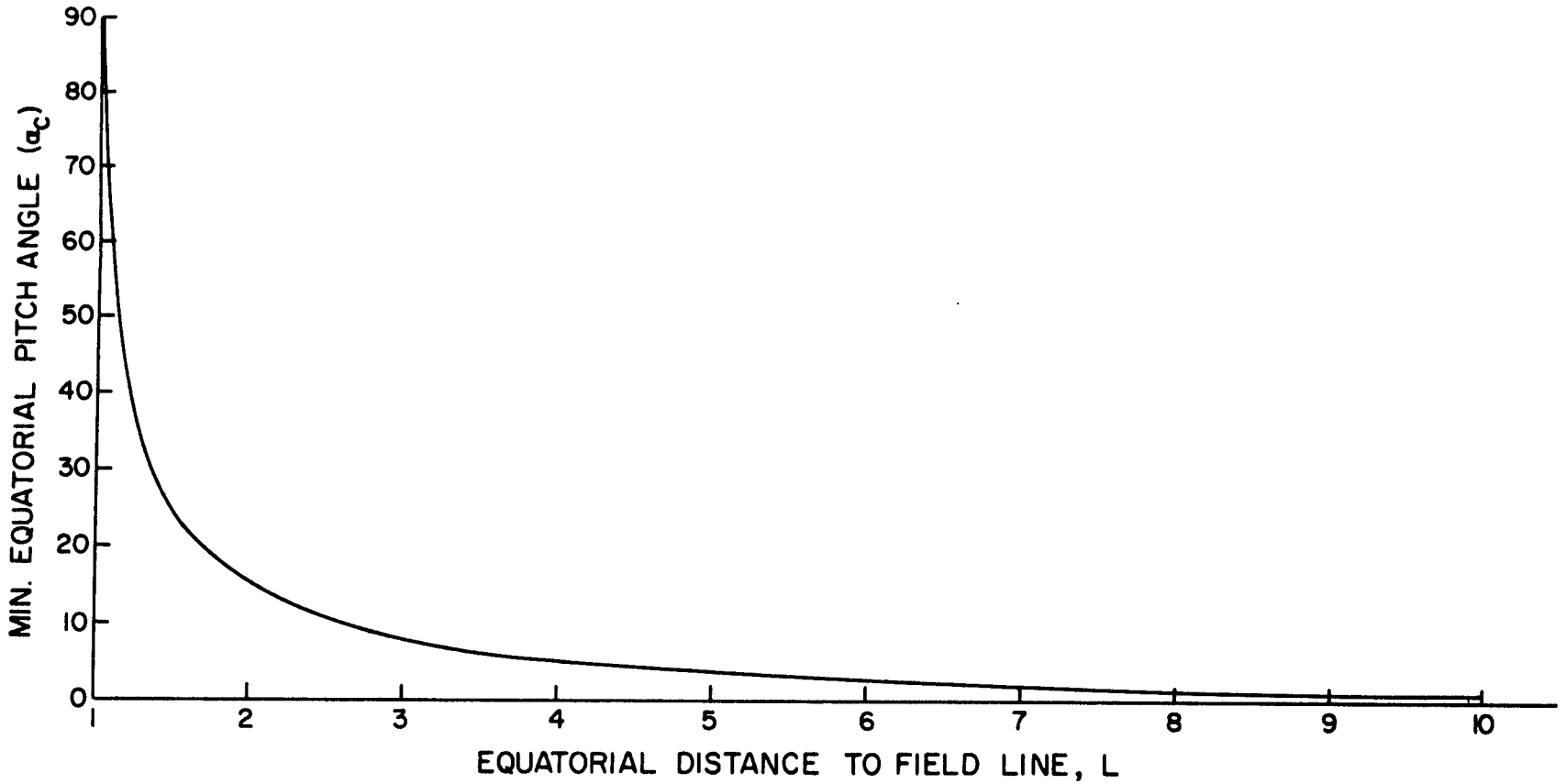

Figure 9

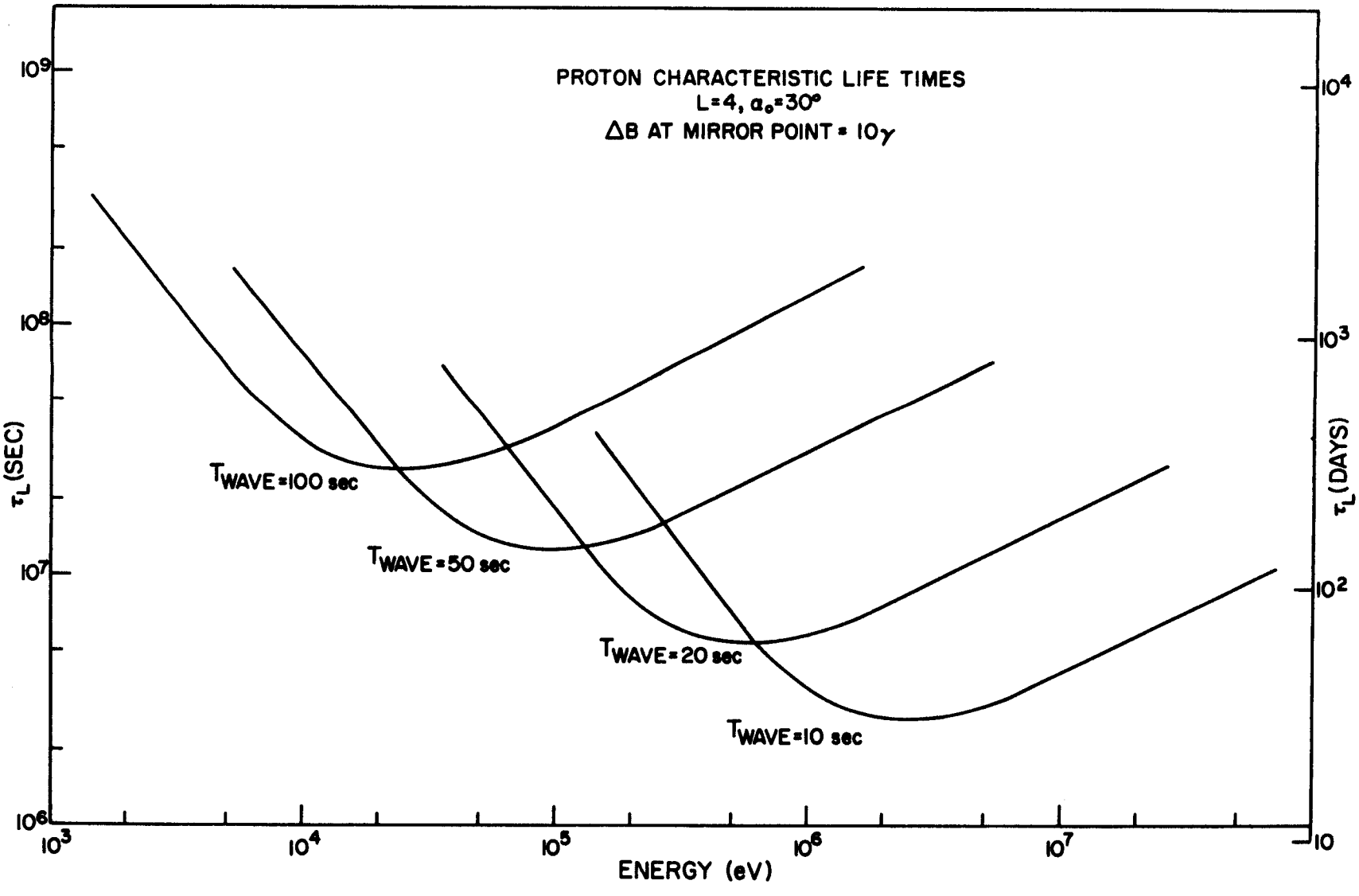
PROTON CHARACTERISTIC LIFE TIMES
L=4, α_o=30°
ΔB AT MIRROR POINT = 10γ
T_{WAVE}=100 sec
T_{WAVE}=50 sec
T_{WAVE}=20 sec
T_{WAVE}=10 sec
τ_L(SEC)
τ_L(DAYS)
ENERGY (eV)
10^9
10^8
10^7
10^6
10^4
10^3
10^2
10
10^3
10^4
10^5
10^6
10^7

Figure 10

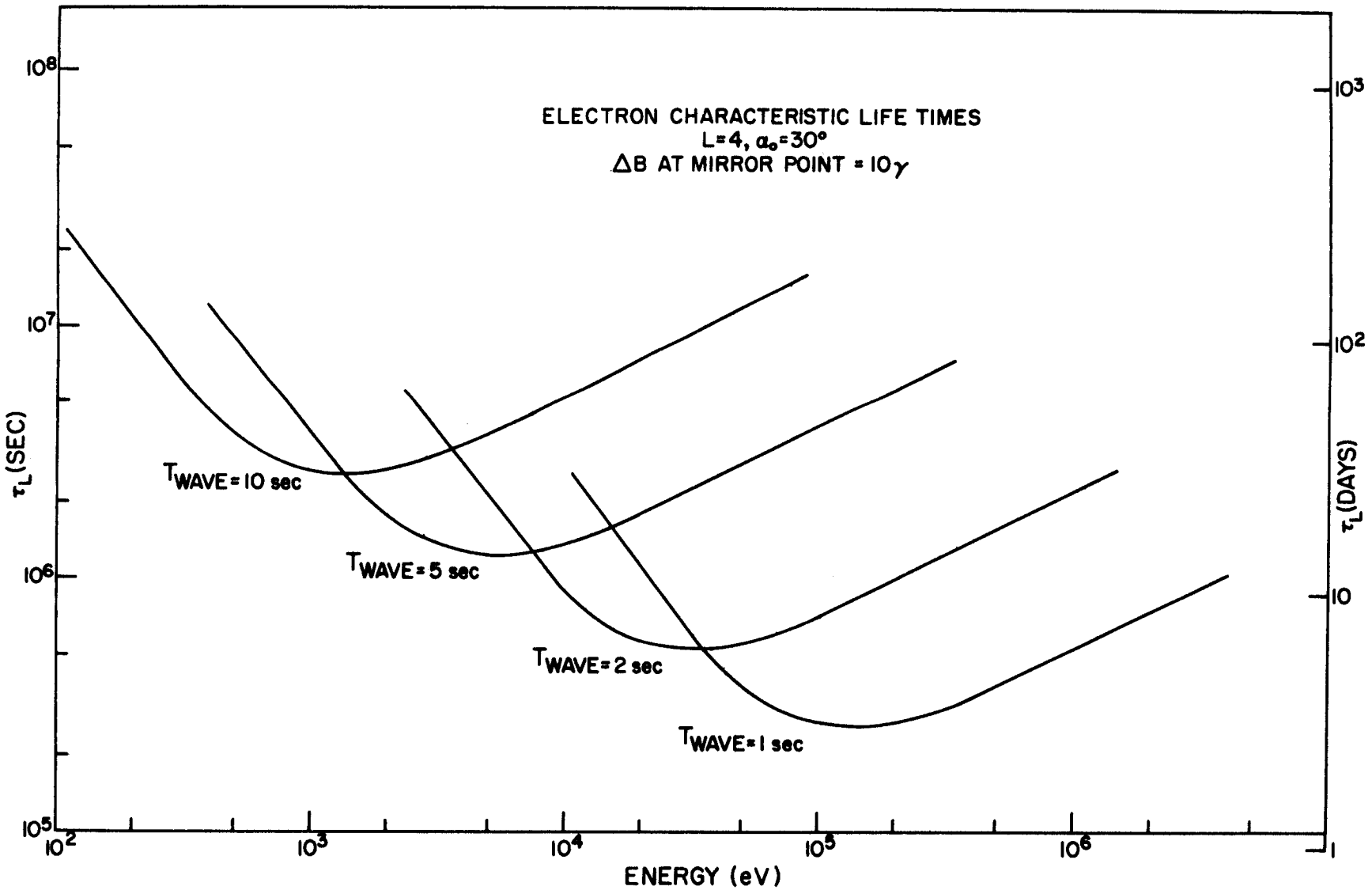
ELECTRON CHARACTERISTIC LIFE TIMES
L=4, α_o=30°
ΔB AT MIRROR POINT = 10γ
T_{WAVE}=10 sec
T_{WAVE}=5 sec
T_{WAVE}=2 sec
T_{WAVE}=1 sec
τ_L(SEC)
τ_L(DAYS)
ENERGY (eV)
10^8
10^7
10^6
10^5
10^3
10^2
10
1
10^2
10^3
10^4
10^5
10^6

Figure 11

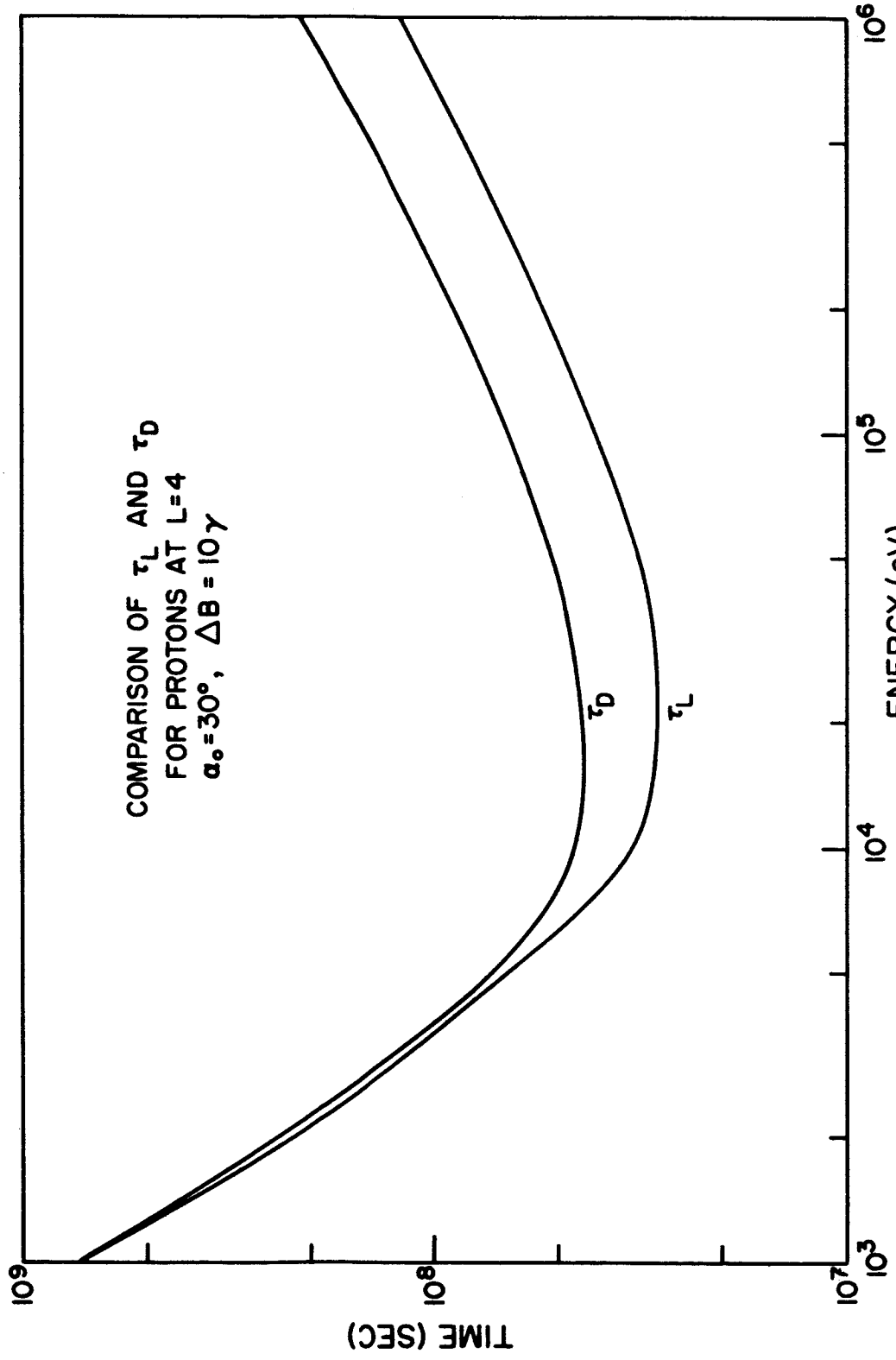
COMPARISON OF τ_L AND τ_D
FOR PROTONS AT L=4
α_o=30°, $\Delta B = 10\gamma$
τ_D
τ_L
TIME (SEC)
ENERGY (eV)
10^9
10^8
10^7
10^3
10^4
10^5
10^6

Figure 12

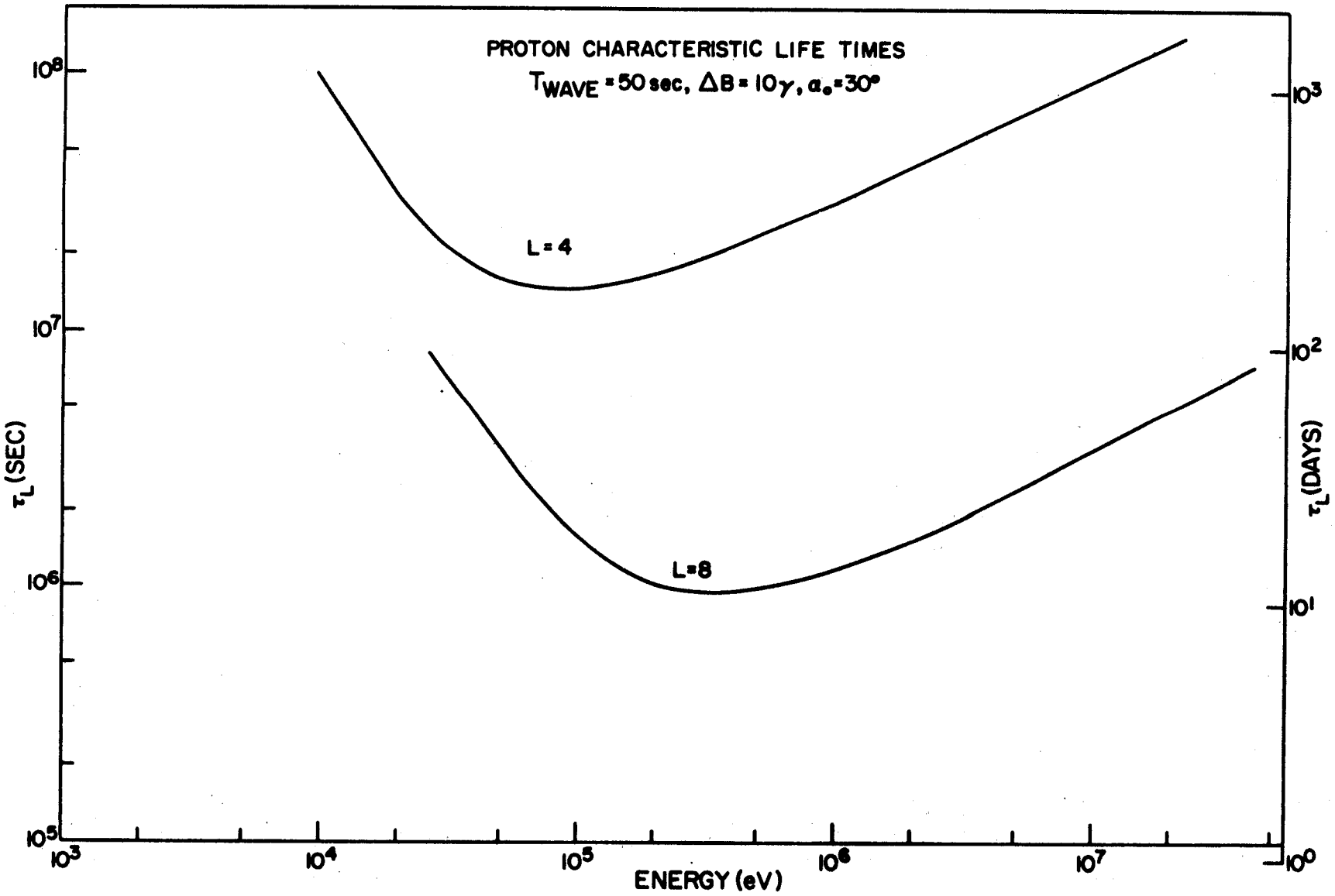
PROTON CHARACTERISTIC LIFE TIMES
T_{WAVE} = 50 sec, ΔB = 10γ, α_o = 30°
L = 4
L = 8
τ_L (SEC)
τ_L (DAYS)
ENERGY (eV)
10^8
10^7
10^6
10^5
10^3
10^2
10^1
10^0
10^3
10^4
10^5
10^6
10^7

Figure 13

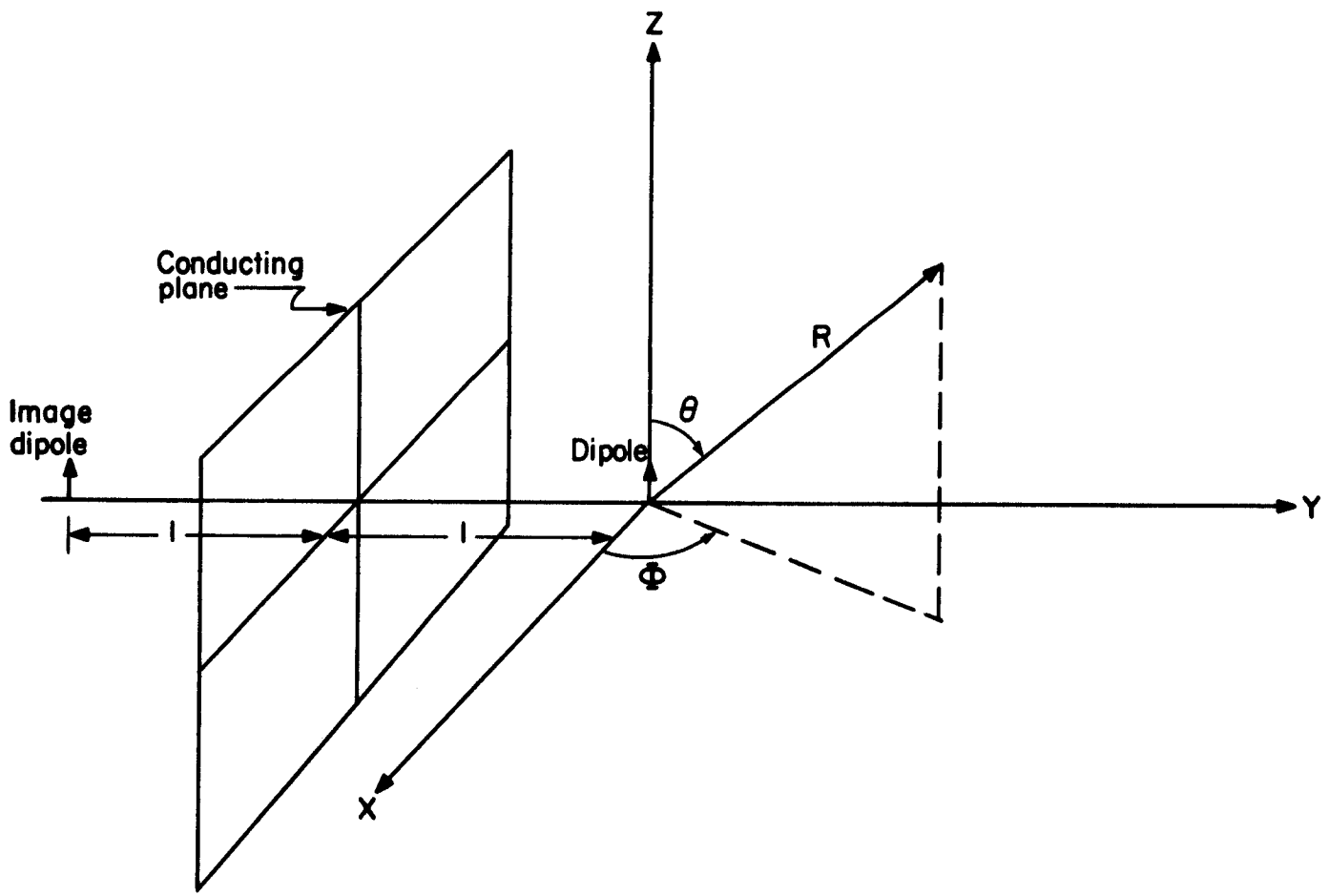

SUDDEN DISTURBANCE MODEL

Figure 14

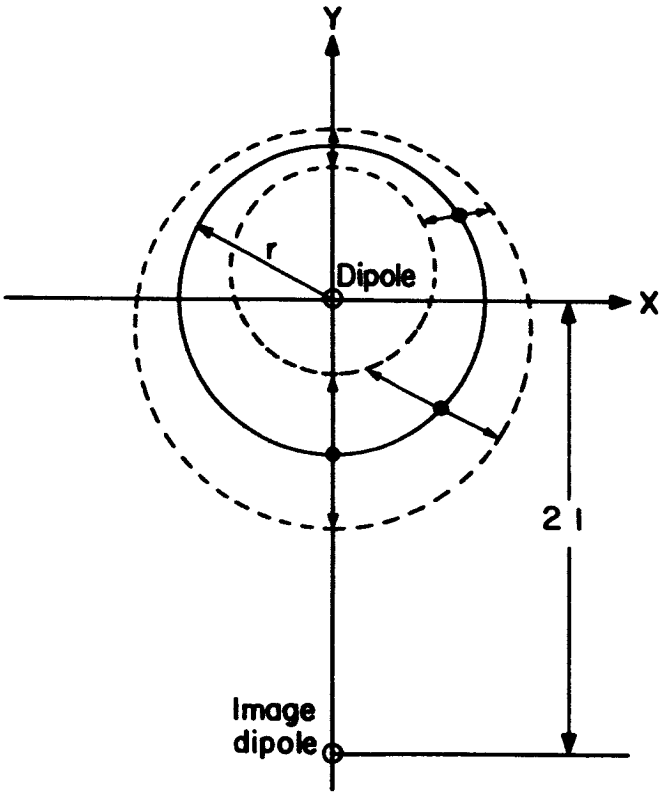

DISPLACEMENT OF MAGNETIC FIELD
LINES IN SINUSOIDAL MODEL

Figure 15

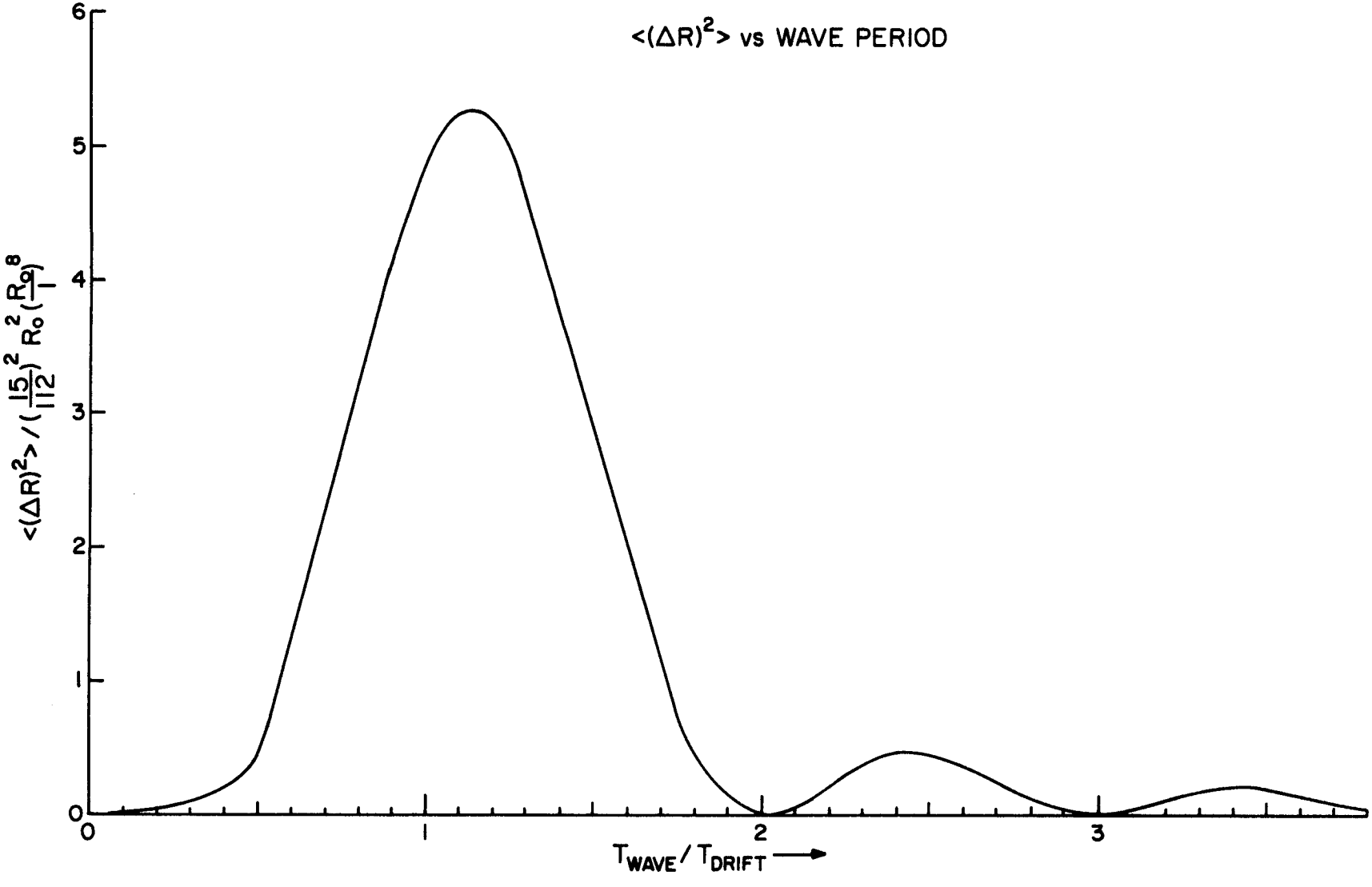
<(ΔR)²> vs WAVE PERIOD
<(ΔR)²> / (15/112)² R₀² (R₀/1)⁸
0
1
2
3
4
5
6
0
1
2
3
T_WAVE / T_DRIFT

Figure 16

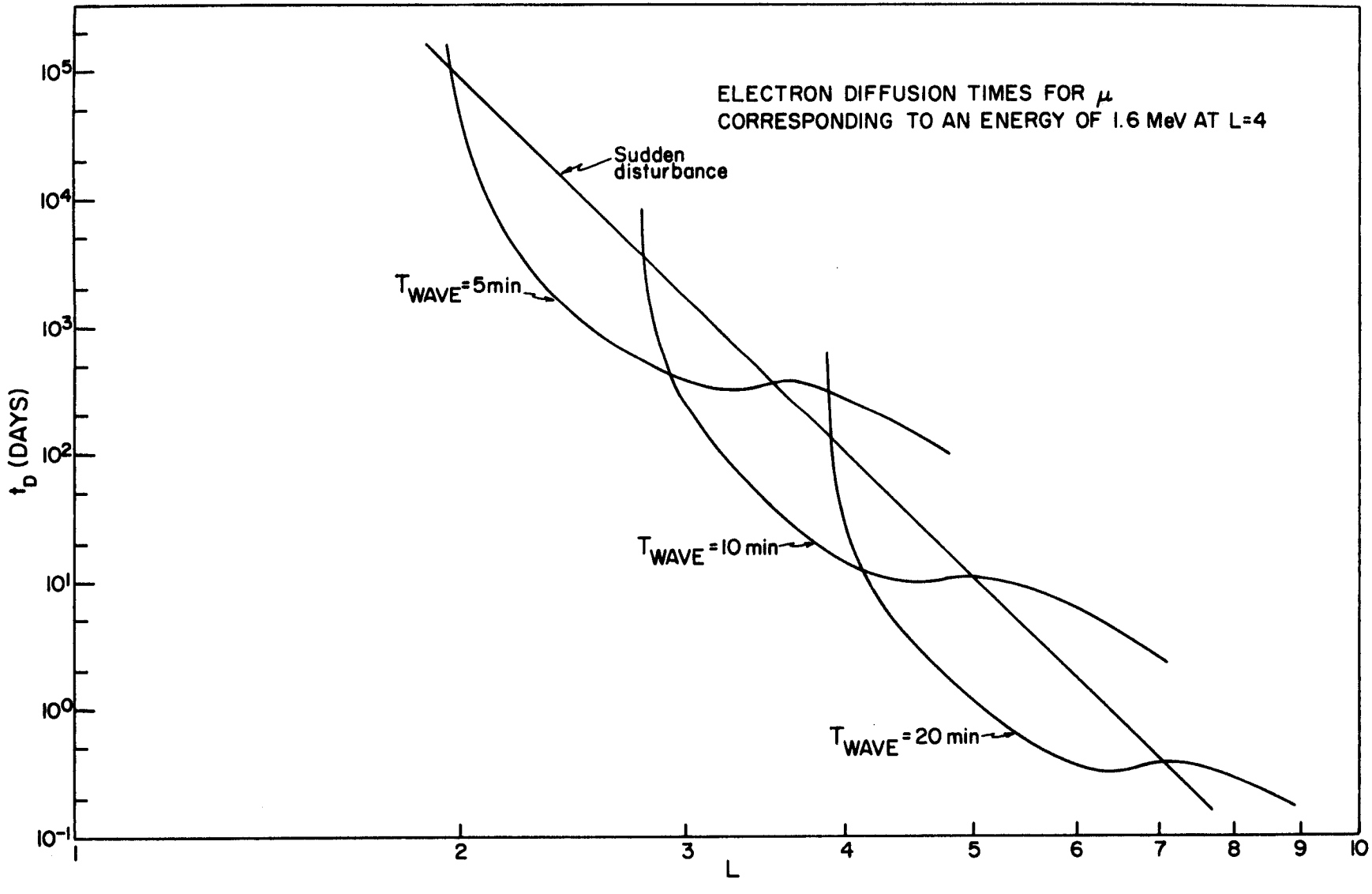
ELECTRON DIFFUSION TIMES FOR μ
CORRESPONDING TO AN ENERGY OF 1.6 MeV AT L=4
Sudden disturbance
T_WAVE = 5 min
T_WAVE = 10 min
T_WAVE = 20 min
t_D (DAYS)
10^5
10^4
10^3
10^2
10^1
10^0
10^-1
1
2
3
4
5
6
7
8
9
10
L

Figure 17